Shahrood University of Technology

Journal of Mining and Environment (JME)

Journal homepage: www.jme.shahroodut.ac.ir

Iranian Society of Mining Engineering (IRSME)

Data-Driven Prediction of Rock Brittleness Using Machine Learning and Advanced Optimization Algorithms

Shirin jahanmiri[1], Ali Aalianvari[1,2*], Majid Noorian-Bidgoli[1], and Jamal Rostami[3]

1. Department of Mining Engineering, University of Kashan, Kashan, Iran
2. Department of Mining and Environmental Engineering, Faculty of Engineering, Tarbiat Modares University
3. Department of Mining Engineering, Colorado School of Mines, Golden, Colorado, USA

Article Info

Received 6 May 2026
Received in Revised form 14 June 2026
Accepted 7 August 2026
Published online 8 August 2026

DOI: 10.22044/jme.2026.17675.3514

Keywords

Rock Brittleness Assessment
Tunnel Engineering
Artificial Rabbit Optimization
Crayfish Optimization Algorithm
Machine Learning Techniques

Abstract

Accurate evaluation of rock brittleness is essential in many rock engineering applications, particularly in tunneling and underground excavation, where brittleness significantly influences rock fragmentation, cutting efficiency, and tool wear. However, direct measurement of brittleness is often difficult, time-consuming, and costly. Therefore, developing reliable predictive models based on commonly available mechanical properties can provide valuable support for engineering practice. In this study, several intelligent computational approaches were employed to predict the rock brittleness index (B) using two key rock mechanical parameters: Uniaxial Compressive Strength (UCS) and Tensile Strength (TS). A comprehensive dataset consisting of 854 records from 23 different rock types was compiled from previously published experimental studies. Four advanced modeling techniques—Artificial Rabbits Optimization (ARO), Crayfish Optimization Algorithm (COA), Grey Wolf Optimizer (GWO), and Gene Expression Programming (GEP)—were implemented and compared to evaluate their capability in predicting rock brittleness. Model performance was assessed using statistical indicators including the coefficient of determination (R^2) and the mean absolute error (MAE) for both training and testing datasets. The results indicated that all models were able to capture the nonlinear relationship between the input variables and the brittleness index. Among them, the ARO model demonstrated the highest predictive accuracy, achieving approximately $R^2 = 0.93$ for the training dataset and $R^2 = 0.94$ for the testing dataset, with the lowest prediction errors. The GWO and GEP models also produced reliable results, while the COA model showed slightly lower predictive capability. The findings of this study highlight the effectiveness of nature-inspired optimization algorithms and evolutionary computation techniques for modeling complex rock engineering properties. The developed models provide a practical and efficient tool for estimating rock brittleness in situations where direct laboratory measurements are unavailable, thereby supporting improved decision-making in tunneling and rock excavation projects.

Abbreviations

ARO – Artificial Rabbit Optimization

COA – Crayfish Optimization Algorithm

GWO – Grey Wolf Optimization

GEP – Gene Expression Programming

RMSE – Root Mean Squared Error

MAE – Mean Absolute Error

MSE – Mean Squared Error

MAPE – Mean Absolute Percentage Error

SMAPE – Symmetric Mean Absolute Percentage Error

MBD – Mean Bias Deviation

TBM – Tunnel Boring Machine

Corresponding author: a.aalianvari@modares.ac.ir (A.Aalianvari)

1. Introduction

Rock brittleness plays a pivotal role in tunnel engineering[1], influencing excavation techniques, structural stability, and overall safety. Brittleness is the tendency of a rock to fracture or fail under stress without significant prior deformation[2]. This characteristic is vital for engineers to understand and quantify, as it directly impacts the selection of excavation methods, the design of support systems, and the long-term stability of tunnel structures[3]. Proper assessment of rock brittleness is, therefore, a crucial step in the planning and execution of tunnel projects[4]. The traditional assessment of rock brittleness involves various experimental techniques such as punch penetration tests, uniaxial compressive strength tests, and Brazilian disc tests[5,6]. The brittleness of the rock mass in tunnel engineering influences several critical factors[7–9]. Firstly, it affects the excavation methods that can be used. Highly brittle rocks are prone to fragmentation, necessitating specialized excavation techniques such as controlled blasting or softer mechanical methods to manage the increased risk of rock breakage[10]. In some cases, brittleness may require adopting slower or more careful excavation methods to avoid excessive fracturing, which can compromise tunnel integrity[11]. Secondly, the brittleness of rock has significant implications for the design of support systems. Tunnels excavated in brittle rock may require enhanced support mechanisms, such as rock bolts, shotcrete, and reinforced linings, to ensure stability and prevent collapse[12]. Without appropriate support, brittle rock is more susceptible to spalling and rock bursts, especially under high in-situ stress conditions[13]. Therefore, accurately assessing brittleness helps engineers design safer and more effective support systems tailored to the specific rock conditions of a tunnel[14]. Thirdly, safety considerations are paramount in tunnel engineering, and the brittleness of the rock directly impacts the safety of both the construction process and the tunnel's long-term use. An accurate assessment of rock brittleness allows engineers to design safer excavation strategies and support systems, reducing the likelihood of tunnel failures. By understanding the brittleness of the rock, engineers can implement measures to mitigate risks, such as adjusting excavation techniques or increasing support in critical areas[15]. This proactive approach not only enhances the safety of workers during construction but also contributes to the long-term stability of the tunnel, ensuring the safety of its users.

In recent years, advancements in intelligent methods and technologies have significantly enhanced the ability to assess and analyze rock brittleness. Table 1 and figure 1 presents a summary of theoretical methods for predicting the rock brittleness index.

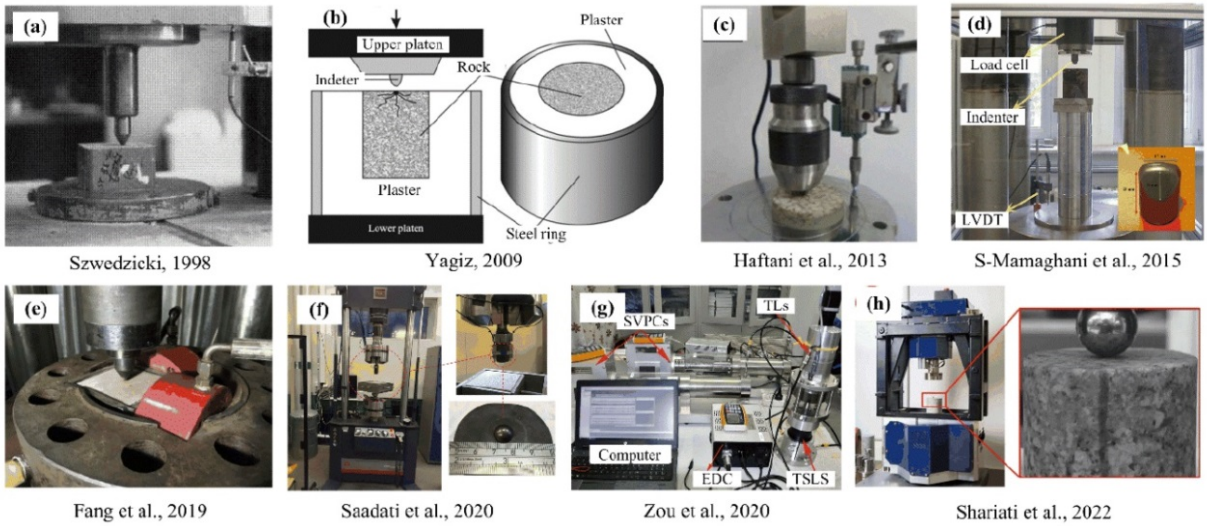

Figure 1. Examples of test devices for penetration testing [29–36]

Table 1. Summary of theoretical methods for predicting rock brittleness index

Researcher	Year	Objective	Achievement	Ref.
Meng et al.	2015	Rock brittleness based on stress-strain curves	Proposed an evaluation method	[16]
Feng et al.	2018	Static and dynamic Young & modulus and Poisson& s ratio based on rock elastic wave theory	Reservoir classification based on brittleness	[17]
Dehkordi	2019	New empirical equations to predict rock mass deformation modulus using brittleness indices	Utilized the Hooke and Diederichs approach to estimate the deformation modulus, considering factors such as intact rock elastic modulus, disturbance factor, and GSI	[18]
Jiang et al.	2022	A mechanical damage model to simulate the fracture process of frozen rocks based on statistical damage theory, Hoek-Brown criterion, and strain difference function	A new brittleness index for frozen rocks using the energy method based on triaxial tests on saturated red sandstones under different low temperatures to investigate the mechanical properties and brittleness of frozen rocks	[19]
Cheng et al.	2022	A reservoir brittleness prediction method based on the Mohr-Coulomb failure criterion and in-situ stress principle	Mathematical relationship between rock mechanical properties and in-situ stress, considering parameters such as Poisson & s ratio, overburden pressure, maximum horizontal stress, and minimum horizontal stress	[20]
Zhong et al.	2023	A new index	High rock brittleness implies high elastic energy	[21]
Xu et al.	2022	Systematization of common brittleness evaluation methods	The effect of characteristics of common brittleness indices on different rock samples based on the stress-strain curve	[22]
Gui et al.	2022	Evaluation of the anisotropy of the brittleness index for shale	The shale brittleness index showed specific anisotropy consistent with uniaxial compression test results	[23]
Gao et al.	2022	Based on pre-peak crack initiation and stress drop characteristics	Effects of confining pressures and different loading modes on rock brittleness	[24]
Yang et al.	2022	Oliver and Pharr method and energy method	Nano-indentation tests on the shale surface to obtain mechanical properties	[25]
Xu et al.	2022	Rock thermal damage constitutive model based on Lemaitre equivalent strain hypothesis and energy dissipation theory	Change in elastic modulus to define thermal damage (DT) and rock damage evolution curves at different temperatures	[26]
Gao et al.	2023	Feasibility of the method using granite, sandstone, and marble test data under various conditions	Proposed a brittleness evaluation method based on rock statistical damage constitutive parameters	[27]
Zheng et al.	2023	Based on energy conversion characteristics after the peak of rock under true triaxial stresses	The proposed evaluation index reveals the intrinsic driving nature of rock brittleness fracture from an energy perspective	[28]

These methods utilize data analytics, machine learning, and artificial intelligence (AI) to improve the accuracy and efficiency of brittleness assessments. By integrating data from multiple sources, such as field tests and laboratory experiments, data analytics offers a more comprehensive understanding of rock behavior. Machine learning algorithms provide advanced capabilities for predicting rock brittleness based on experimental data. These algorithms can analyze complex datasets, identify underlying patterns, and make accurate predictions about brittleness indices. In the context of rock brittleness assessment, common machine learning techniques include regression analysis, which models the relationship between rock properties and the brittleness index, classification algorithms to categorize rocks into different brittleness classes, and clustering methods to group similar rock types and assess their brittleness characteristics. These techniques enable more nuanced and accurate predictions, which are invaluable for planning and decision-making in tunnel engineering.

Artificial intelligence methods, including neural networks and expert systems, have the potential to revolutionize rock brittleness assessment. AI can integrate experimental data with historical knowledge and real-time monitoring to provide dynamic and adaptive solutions[37]. For instance, AI-based systems can continuously update brittleness models as new data becomes available, improving the accuracy and reliability of predictions. This dynamic capability is particularly useful in tunnel engineering, where real-time adjustments may be needed based on evolving conditions during excavation.

AI-based systems further refine brittleness assessments and provide real-time updates. Key applications of AI in this context include adaptive models that update dynamically as new data is acquired and decision support systems that provide recommendations for excavation methods and support systems based on real-time data.

These AI-driven systems enhance the ability to respond to changing conditions during tunnel excavation, improving both the efficiency and safety of the construction process. A review of historical methods reveals the evolution of brittleness assessment techniques, from early empirical methods to modern analytical approaches. Traditional methods, such as punch penetration testing and laboratory strength tests, have laid the foundation for more advanced techniques by providing baseline measurements of rock brittleness. However, these methods have limitations in terms of the time, cost, and effort required to perform extensive testing and analysis. Recent literature highlights the integration of data analytics, machine learning, and AI in geotechnical engineering, demonstrating the effectiveness of these methods in enhancing the accuracy of rock brittleness assessments and optimizing tunnel design. Studies have shown that intelligent methods can significantly improve the predictive accuracy of brittleness assessments, reduce the time required for analysis, and provide more detailed insights into rock behavior. These advancements have opened new avenues for research and application in tunnel engineering, contributing to the development of safer, more efficient, and cost-effective tunneling methods. In recent years, various metaheuristic algorithms such as genetic algorithms, particle swarm optimization, and grey wolf optimizer (GWO) have been employed to improve the prediction of rock mechanical properties and brittleness indices. These methods are mainly used to optimize model parameters, select informative features, or refine regression coefficients. In this study, we employ two relatively recent metaheuristic algorithms, the Animal Robot Optimizer (ARO) and the Coyote Optimization Algorithm (COA), to hybridize with Gene Expression Programming (GEP) for brittleness prediction. ARO and COA are chosen because they demonstrate strong performance on continuous optimization problems and provide a favorable exploration–exploitation balance, while, to the best of the authors' knowledge, they have not yet been systematically evaluated for rock brittleness prediction.

Case studies illustrate the practical application of intelligent methods in various tunnel projects. Examples include the use of machine learning to predict rock brittleness in specific geological conditions and the integration of AI-based systems for real-time monitoring and decision support. These case studies demonstrate how the combination of traditional experimental methods with intelligent techniques can enhance the assessment of rock brittleness, providing valuable guidance for tunnel design, excavation methods, and support systems. The study aims to develop predictive models by utilizing machine learning algorithms to predict brittleness indices and improve assessment accuracy. It also seeks to enhance data interpretation by applying data analytics to derive actionable insights from experimental results. Furthermore, the study intends to provide practical recommendations for optimizing tunnel design and excavation methods based on integrated brittleness assessments.

The prediction of rock brittleness has attracted considerable attention due to its critical role in tunnel excavation performance and rock fragmentation behavior. Previous studies have applied various machine learning approaches such as artificial neural networks, support vector machines, and gene expression programming to model brittleness indices using rock mechanical properties. For instance, several studies have reported prediction accuracies ranging from R^2 values of approximately 0.80–0.92 depending on the dataset and modeling approach.

Despite these advances, the application of recent metaheuristic optimization algorithms, such as Artificial Rabbit Optimization (ARO) and Crayfish Optimization Algorithm (COA), to brittleness prediction remains largely unexplored. These algorithms have demonstrated strong global search capabilities and improved convergence behavior in complex optimization problems.

Therefore, the present study aims to develop and compare multiple intelligent predictive models for rock brittleness using Gene Expression Programming (GEP), Grey Wolf Optimization (GWO), Crayfish Optimization Algorithm (COA), and Artificial Rabbit Optimization (ARO). The models are trained using a comprehensive dataset compiled from previous studies and validated across 23 different rock types, with performance evaluated using multiple statistical metrics. This comparative framework provides new insights into the suitability of advanced optimization algorithms for brittleness prediction in tunnel engineering.

This study aims to advance the field of rock brittleness assessment by integrating traditional experimental methods with modern intelligent techniques. The integration of these methods will enable a more comprehensive understanding of rock behavior, facilitating better decision-making and risk management in tunnel projects. Future research will focus on expanding the application

of intelligent methods, validating findings through field studies, and exploring new technologies for enhancing brittleness assessments. The ultimate goal is to develop more robust and adaptive solutions for managing the challenges associated with rock brittleness in tunnel projects. By advancing the state of knowledge in this field, the study aims to contribute to the development of safer, more efficient, and cost-effective tunneling methods that can be applied in various geological conditions, ultimately improving the overall success and sustainability of tunnel engineering projects.

2. Methodology

This study employs several advanced artificial intelligence and optimization techniques to develop predictive models for estimating the rock brittleness index (B) based on two key input parameters: Uniaxial Compressive Strength (UCS) and Tensile Strength (TS). Four intelligent modeling approaches were implemented and compared, namely Gene Expression Programming (GEP), Grey Wolf Optimizer (GWO), Crayfish Optimization Algorithm (COA), and Artificial Rabbits Optimization (ARO). These techniques were selected due to their strong capability to capture complex nonlinear relationships between input and output variables.

The overall modeling framework consists of data preparation, model development, parameter optimization, and performance evaluation. The compiled dataset was divided into training and testing subsets. The training dataset was used to construct and optimize the predictive models, while the testing dataset was used to assess their generalization capability.

Figure 2 illustrates the methodology of the present study for predicting the rock brittleness index.

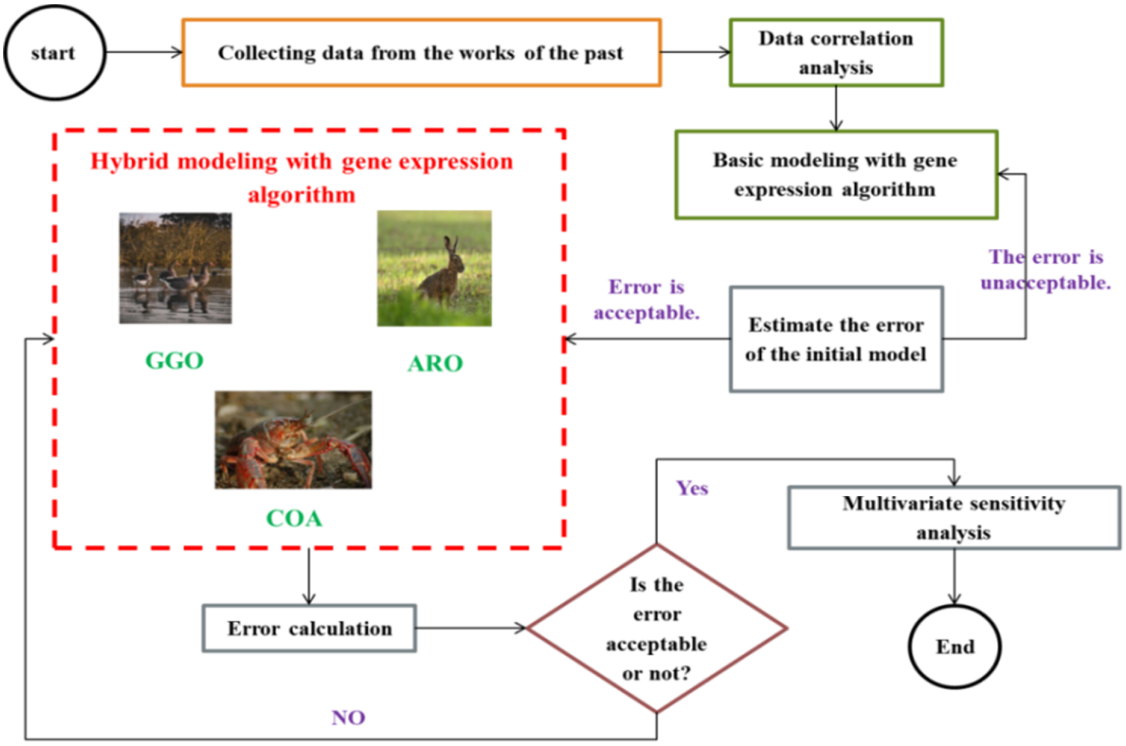

Figure 2. Classification of studies conducted in the field of rock brittleness index

3. Data Collection

The data used in the present study were compiled from previous research conducted by various scholars and further supported by [38–55]. These studies encompass 23 different rock types, providing a broad and representative basis for brittleness evaluation in tunneling applications.

A total of 854 records were collected from the available dataset. The input variables used in this study were:

- Uniaxial compressive strength (UCS)
- Tensile strength (TS)

The target variable was the rock brittleness index.

To ensure model evaluation, the dataset was divided into training and testing subsets. In the revised and consistent version, the dataset is assumed to be split into:

- 70% training
- 15% validation
- 15% testing

This division supports fair model calibration and independent performance assessment.

The compiled dataset involves three primary parameters: Uniaxial Compressive Strength (UCS), Tensile Strength (TS), and the Brittleness Index (B). These variables are fundamental indicators of rock mechanical behavior and are widely used in rock mechanics and tunneling design. UCS characterizes the compressive load-bearing capacity of intact rock, TS reflects its resistance to tensile failure, and the brittleness index B is used to quantify the tendency of a rock to fail suddenly with limited plastic deformation. Together, these parameters provide an integrated description of rock strength and failure characteristics.

A statistical summary of the variables used in this study is provided in Table 2, including the minimum, first quartile (Q1), median, third quartile (Q3), maximum, and mean values for UCS, TS, and B. This statistical overview highlights the wide range of rock strengths and brittleness characteristics represented in the dataset, thereby supporting the development of robust data-driven models that can generalize across different rock types and geological settings.

A statistical summary of the input parameters is presented in Table 2, detailing the minimum, maximum, average, and mode values for the dataset.

Table 2. Statistical parameters of the dataset used in this study.

Type	Variable	Num.	Mean	Min	Q1	Median	Q3	Max
Input	Tensile Strength	854	13.63	0.20	4.40	6.96	10.77	224.00
	Uniaxial Compressive Strength	854	114.09	2	45.59	84.41	155.95	559.20
Output	Rock Brittleness Index	854	15.59	0.82	9.365	13.27	17.52	89.14

The comprehensive dataset, comprising 854 individual data records collected from extensive experimental and literature sources, was then integrated with advanced intelligent analytical methods. These include data analytics, machine learning (ML), and artificial intelligence (AI) techniques, which were employed to develop predictive models for the brittleness index of rocks. The primary objective of this integration was to identify complex, non-linear relationships between UCS, TS, and B, and to derive actionable insights for rock engineering applications. The large volume and diversity of the dataset, covering a wide spectrum of rock types and mechanical properties, facilitated effective training and validation of the ML models and improved their accuracy and generalizability across different geological conditions.

Figure 3 illustrates the frequency of the parameters used.

The reason for selecting the tensile strength and compressive strength parameters is that the main brittleness indices (B1 to B13) are based on strength parameters [84]. These parameters are easily measurable in the laboratory, and in all studies where data were available, these two primary parameters existed. Thus, indices B1 to B5, which are likely the simplest brittleness indices, are expressed as follows:

$$B_1 = \frac{\sigma_c}{\sigma_t} \quad (1)$$

$$B_2 = \frac{(\sigma_c - \sigma_t)}{(\sigma_c + \sigma_t)} \quad (2)$$

$$B_3 = \frac{(\sigma_c + \sigma_t)}{2} \quad (3)$$

$$B_4 = \frac{\sigma_c \sigma_t}{2} \quad (4)$$

$$B_5 = \sqrt{\frac{\sigma_c \sigma_t}{2}} \quad (5)$$

In the above equations, σ_c represents the uniaxial compressive strength (UCS) and σ_t represents the Brazilian tensile strength. The present study was conducted based on five main indices.

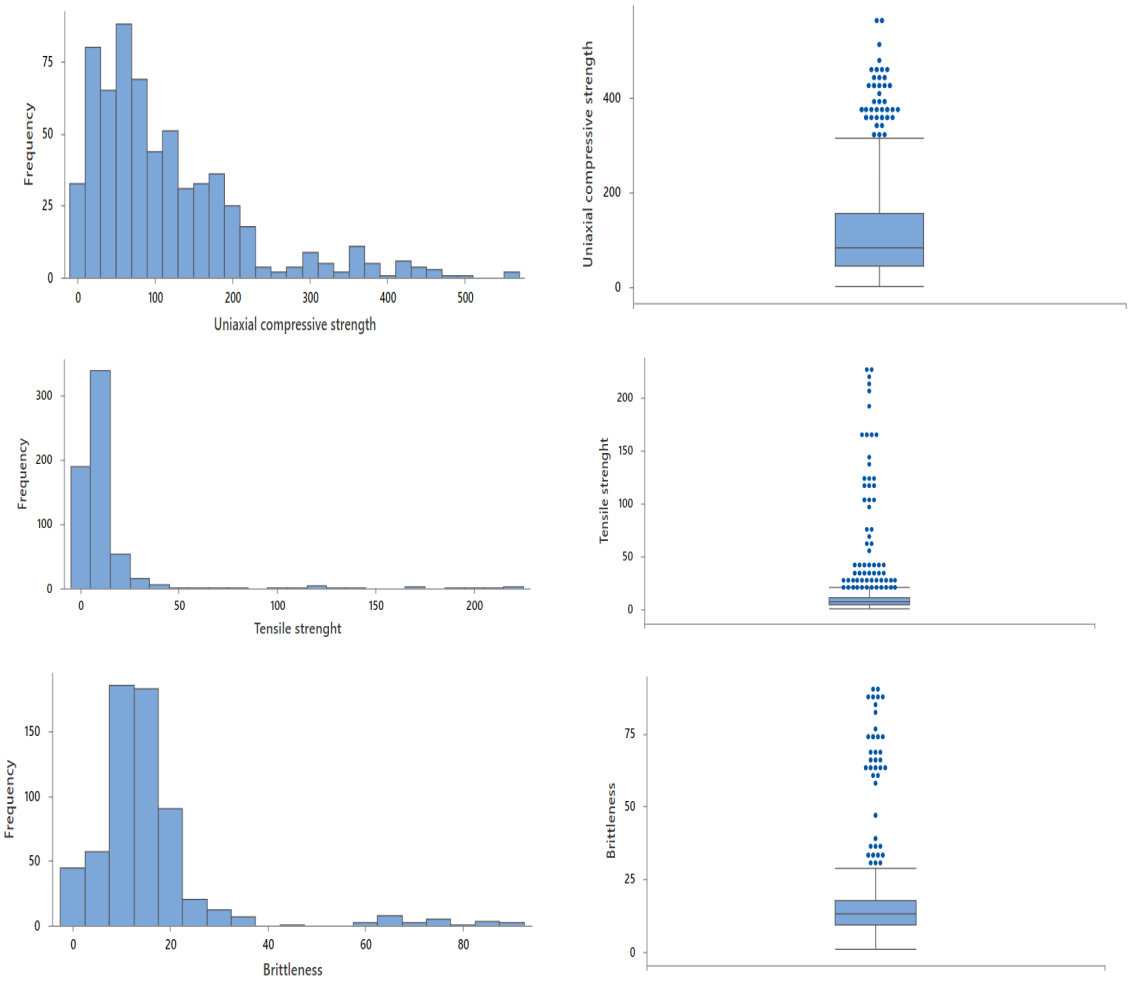

Figure 3. Frequency of the parameters used in the present study, classified by type

Figure 4 illustrates the correlation of the parameters.

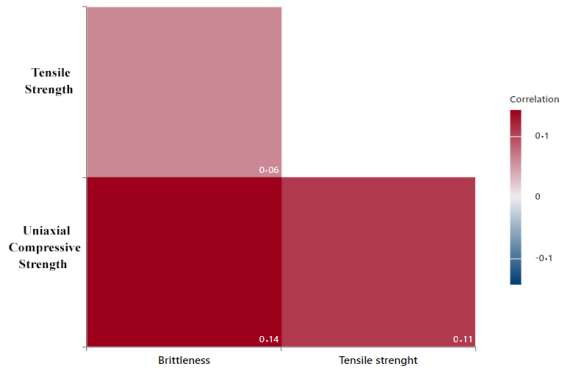

Figure 4. Correlation of the parameters used in modeling

4. Integration with Intelligent Methods

For the development and assessment of the proposed predictive models, the compiled dataset was divided into two distinct subsets: a **training set** and a **testing set**. The training set was used for model calibration, parameter optimization, and learning the underlying relationships between UCS, TS, and the brittleness index B. The testing set was held out and employed exclusively for an **independent evaluation** of the models' generalization capability.

The performance of all models (ARO, COA, GWO, and GEP) was evaluated on both the training and testing datasets using standard statistical indicators, including the **coefficient of determination (R^2)** and the **Mean Absolute Error (MAE)**. For example, the ARO model achieved an R^2 of 0.93 with an MAE of 1.06 on the training set and an R^2 of 0.94 with an MAE of 0.88 on the testing set. Similarly, the GWO and GEP models also showed high and consistent performance across both phases, whereas the COA model exhibited slightly lower but still competitive prediction capability. Reporting these metrics for both training and testing subsets

demonstrates that the developed models are not only accurate but also robust and capable of providing reliable predictions of rock brittleness for unseen data.

4.1. Gene expression programming (GEP)

Figure 5 [56] shows the flowchart of a gene expression programming (GEP) method. The creation of random chromosomes for the starting population is the first step in this procedure. After that, each person's fitness is assessed based on the expression of their chromosomes [57]. Then, individuals are chosen according to how well they are suited for modified reproduction, which results in children with novel features[58]. These individuals of the new generation go through a consistent development process that includes modified reproduction, exposure to a selective environment, and genome expression. Until a solution is discovered, this procedure is repeated for a predetermined number of generations [59]. It is important to remember that reproduction entails both replication and the activity of genetic operators that might produce genetic variation[37]. During reproduction, the genome is copied and passed on to the next generation. It is evident that reproduction alone cannot create diversity; genetic diversity is introduced into the population only through the action of genetic operators. These operators randomly select some chromosomes that need to be modified. Therefore, in GEP, a chromosome may be modified by one or more operators at a time or may not be changed at all [60].

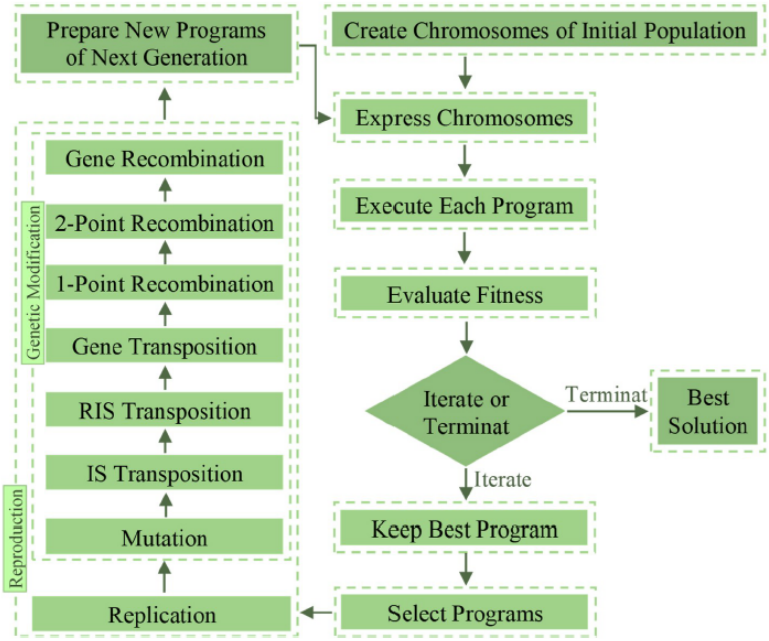

Figure 5. Gene expression algorithm flowchart[61]

4.2. Grey Wolf Optimization Algorithm (GWO)

The GWO algorithm begins by generating several individuals randomly. Each individual represents a solution that may be a candidate solution for the problem [62]. The GWO population is considered to have a size of n, representing a pack of wolves. An objective function, Fn, is selected to evaluate individuals in the group[63]. After calculating the objective function for each individual (wolf) Xi, the best solution (alpha) is selected and denoted as P. The dynamic behavior of GWO algorithm divides all individuals into an exploratory group (1) and an exploitative group (2). The number of solutions in each group is dynamically managed with each iteration according to the best solution. GWO starts with 50% exploration and 50% exploitation in the groups. Then, the number of individuals in the exploration group ($n1$) decreases while the number of individuals in the exploitation group (2) increases. However, if the objective function value of the best solution does not change for three consecutive iterations, the algorithm starts increasing the number of individuals in the exploration group (1) to find another best solution and hopefully avoid local optima[64].

4.3. Optimization Algorithm of Crayfish (COA)

The crayfish is similar to shrimp, with a very firm shell[65]. It belongs to the Crustacea, which includes crustaceans and decapods, in animal classification. Generally, it is considered a key species in freshwater habitats[66]. Crayfish inhabit a wide range of freshwater habitats, from lakes, rivers, and streams to cave pools, temporary ponds, and even seasonal moist areas[67]. They have a habit of digging burrows and emerging at night. There are over 600 recorded species of freshwater crayfish worldwide, capable of digging irrespective of geographical location or habitat. All crayfish have burrows, but the shape and function of these burrows vary among species. This variation in crayfish classification based on cave ecology[68]. Crayfish dig burrows to prevent natural enemies and summer heat. Not only that, but burrows can also be used to avoid predators, prevent drying out, search for food, and care for offspring. Crayfish are a type of aquatic creature that can tolerate a wide range of temperatures. They can adapt to different climatic conditions, provide commercial feed, and be inexpensive. After six months of cultivation, crayfish can grow to 40-60 grams. After years of research, deeper studies have been conducted on crayfish growth[69]. Like all decapods, temperature changes in the living environment can either prolong or shorten the growth rate of crayfish[70]. Therefore, temperature has a significant impact on crayfish survival. They can survive between 11 and 44 degrees Celsius, but that doesn't mean it's suitable for their growth. The optimal temperature for crayfish growth is between 15 and 30 degrees Celsius, and the most suitable temperature for survival is 25 degrees Celsius. If the water temperature is too low, it can easily cause crayfish to eat less or not at all, thereby affecting their growth or even causing their death[71]. When the water temperature is too high, crayfish can easily be brought to the shore without oxygen and even die. A schematic diagram of a crayfish is shown in Figure 6. Crayfish are omnivorous animals that can feed on various grains, cakes, vegetables, terrestrial plants, aquatic plants, epiphytic algae, zooplankton, aquatic insects, small benthos, and animal carcasses[72]. When crayfish are hunting, they usually catch large prey with their claws and tear it apart before sending it to their second and third legs to hold and chew. For small prey, they use their second and third legs directly for holding and pecking, as shown in Figure 7. In the Crayfish Optimization Algorithm (COA), each crayfish represents a candidate solution xi. The algorithm mimics key behaviors such as random walking, attraction.repulsion, and backward movement to escape predators. The position update for a crayfish at iteration t can be generally expressed as[61]:

$$\mathbf{x}_i^{t+1} = \mathbf{x}_i^t + \gamma_t \mathbf{A}_i^t \tag{6}$$

Where γt is a control parameter and $\mathbf{A}_i^t$ is a behavior-dependent movement vector that incorporates attraction towards promising regions and repulsion from less favorable areas. The backward movement mechanism enhances the ability of COA to escape local optima by allowing crayfish to retreat from recently visited, suboptimal locations. The full set of update equations and algorithmic steps for COA, including the construction of $\mathbf{A}_i^t$, are presented in detail in the original COA publications, to which the interested reader is referred for implementation-level details.

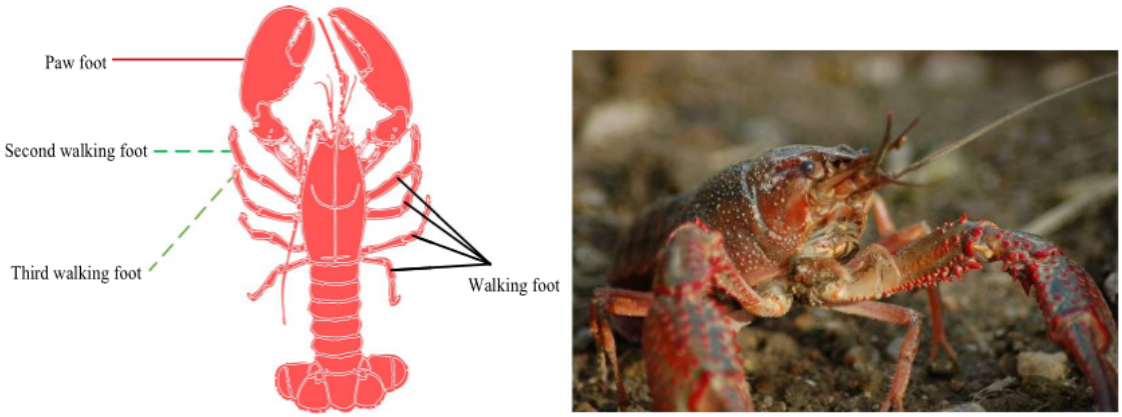

Figure 6. Crab schematic diagram and crab structure diagram[71]

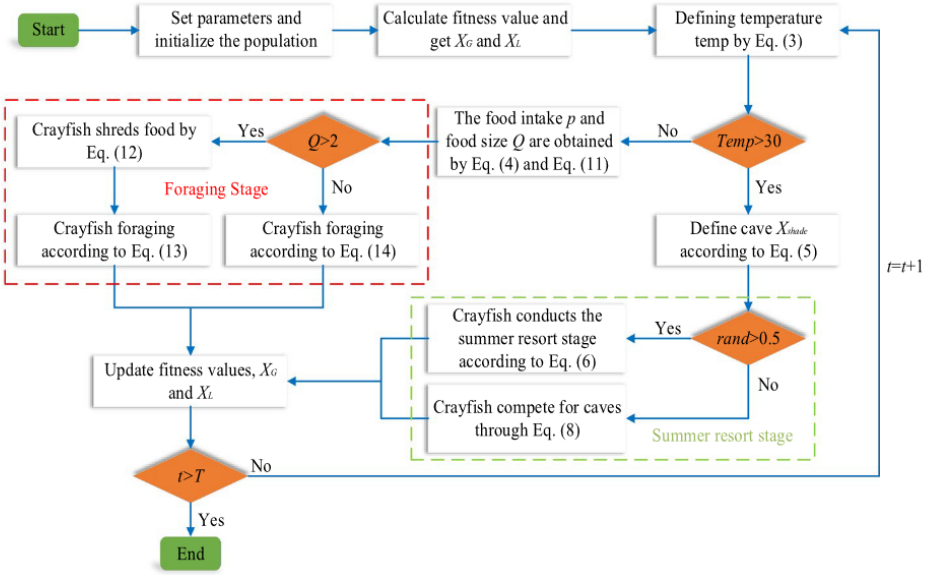

Figure 7. Flowchart of crab optimization algorithm (COA) [66]

4.4. Artificial Rabbit Optimization

The Artificial Rabbit Optimization (ARO) algorithm is introduced in Figure 8 presenting the inspiration and idea behind it. Then, mathematical models for simulating survival strategies are explored[73]. ARO is derived from the survival strategies of rabbits in nature. Like any other species in our evolutionary history, rabbits must evolve to survive[74]. To avoid detection by predators, rabbits do not consume grass near their burrows; they constantly forage away from their nests. Rabbits have a wide field of vision, with most of it dedicated to scanning overhead, enabling them to easily locate food in a large area[75]. This survival strategy of rabbits has widely spread as a common Chinese proverb: "Rabbits don't eat the grass near their burrows[76]. Another survival strategy of rabbits is random hiding. Rabbits are adept at building burrows for their nests. To evade predators, a rabbit digs numerous holes around its burrow and randomly selects one as a refuge from predators[77]. Rabbits have short, strong front legs and powerful muscles and tendons, allowing them to dart quickly[78]. Additionally, they can suddenly stop while running, hop intensely, or backtrack to evade pursuit in a zigzag motion. This survival strategy easily confuses their enemies and helps them evade tracking effectively, potentially increasing the survival chances of rabbits. We will consider this strategy of random concealment as an exploitation[79]. Since rabbits are at the bottom of the food chain and have many predators, they must swiftly escape danger, which depletes their energy. Therefore, rabbits must balance between foraging and random hiding to conserve energy. Mathematically, the Artificial Rabbit Optimization (ARO) algorithm operates on a population of candidate solutions (rabbits) denoted by:

$$X = \{x_1, x_2, ..., x_N\} \tag{7}$$

Where each xi represents a potential solution in the search space. At each iteration t, ARO alternates between a **foraging (exploration)** phase and a **random hiding (exploitation)** phase. In the foraging phase, rabbits move away from their current burrow according to:

$$\mathbf{x}_i^{t+1} = \mathbf{x}_i^t + \alpha_t \mathbf{r}_1 \odot (\mathbf{x}_{\text{best}}^t - \mathbf{x}_i^t) \tag{8}$$

Where αt is a time-decreasing step size, r1 is a random vector in [−1,1], ⊙ denotes element-wise multiplication, and $\mathbf{x}_{\text{best}}^t$ is the best solution found so far. In the random hiding phase, rabbits select one of several candidate hiding places (burrows) around their current position and perform a local exploitation step:

$$\mathbf{x}_i^{t+1} = \mathbf{h}_k^t + \beta_t \mathbf{r}_2 \tag{9}$$

Where $\mathbf{h}_k^t$ is the position of the k-th hiding place chosen randomly from a set of nearby holes, βt controls the exploitation radius, and r2 is a random perturbation vector. The choice between foraging and random hiding is governed by a probability parameter that gradually shifts the

search from global exploration to local exploitation as the iterations proceed.

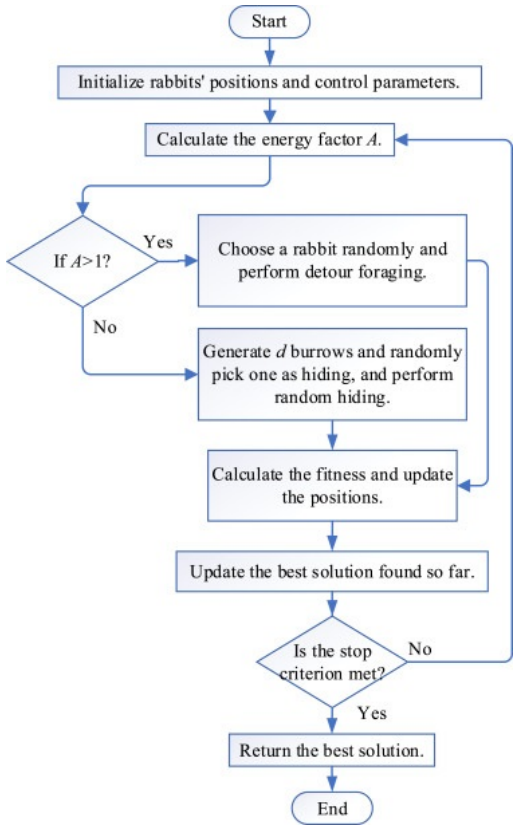

Figure 8. Flowchart of artificial rabbit optimization algorithm (ARO) [73]

5. Modeling

Grey Wolf Optimizer (GWO) was initially examined as a baseline metaheuristic; however, its performance under the tested configurations did not surpass the standard GEP model and was consistently inferior to the ARO–GEP and COA–GEP frameworks. Therefore, detailed GWO results are not reported here in order to focus on the most effective approaches. The database comprising 854 records was randomly divided into three subsets: 70% for training, 15% for validation, and 15% for testing (random seed = 123). All data-dependent statistics used in scaling or in the optimization process (e.g., minimum and maximum values, means, and standard deviations of the inputs and the target brittleness index) were computed exclusively from the training subset. These statistics were then applied to transform the validation and test data, thereby preventing any information leakage from the test set into model training or metaheuristic optimization. The metaheuristic algorithms (ARO and COA) interacted only with the training and validation data during the search process, while the test set was reserved for final performance assessment.

In this study, the Artificial Rabbit Optimization (ARO), Crayfish Optimization Algorithm (COA), Grey Wolf Optimizer (GWO), and Gene Expression Programming (GEP) are implemented as independent, stand-alone models for predicting the rock brittleness factor. Each model is trained and evaluated separately and there is no hybridization or cascading between these approaches (e.g., no ARO–GEP or COA–GEP comparative models). Instead, the algorithms are compared in a parallel benchmarking framework, where their predictive performance on training and testing datasets is assessed using a common set of statistical indicators (MAE, MSE, RMSE, R^2, MAPE, SMAPE, Median AE, Max Error, Explained Variance, and MBD). GEP is specifically employed as a symbolic regression technique that provides an explicit analytical expression for the brittleness factor, while ARO, COA, and GWO serve as metaheuristic optimizers for developing high accuracy predictive models.

To develop and evaluate the predictive models, the compiled dataset of 854 records was randomly divided into training and testing subsets. Specifically, 70% of the data were allocated to the training set and 30% to the testing and validation set (stratified random sampling was not required because the brittleness factor values are continuously distributed and do not exhibit sharp class boundaries). The training subset was used to fit the parameters of the ARO, COA, GWO, and GEP models, while the testing subset was held out and used only for out of sample performance assessment.

Figure 9. illustrates the results of applying the Gene Expression Programming (GEP) algorithm within a decision tree structure. As shown in the figure 9, the algorithm analyzes the input features and their relationships to generate an optimized decision tree that represents the decision-making process in a hierarchical manner. Each node corresponds to a condition or function selected by the algorithm, while the branches indicate how the data are partitioned based on these conditions.

This structure demonstrates the capability of the GEP algorithm to extract meaningful patterns from the data and translate them into interpretable decision rules for prediction or classification tasks. Owing to the evolutionary nature of the algorithm, the final model represents the best-performing decision tree obtained after several generations, achieving the highest accuracy on the dataset used.

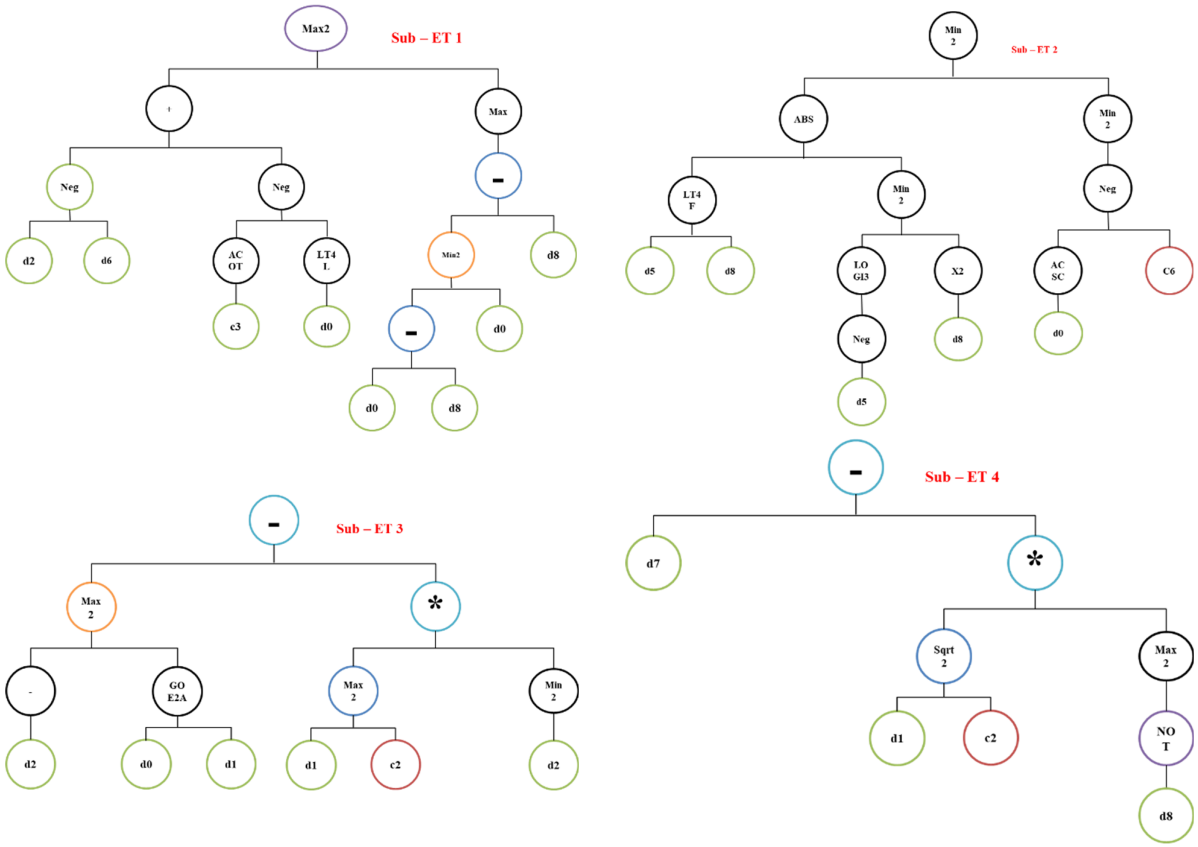

Figure 9. The results of the gene expression algorithm in the decision tree

Table 3 presents the set of parameters used for developing the model based on the Gene Expression Programming (GEP) algorithm. These parameters define the evolutionary settings, structural constraints, and genetic operators that guide the optimization process during model training. The table includes key elements such as population size, number of generations, mutation and recombination rates, as well as the configuration of chromosomes and expression trees. Selecting appropriate parameter values is essential, as they directly influence the convergence speed, model complexity, and overall predictive performance of the GEP-based model. The parameter values were selected based on preliminary experiments and literature recommendations to ensure stable convergence and fair comparison among models.

The parameter values utilized in the GWO algorithm are presented in the table 4. Since the optimization objective was based on the values generated by the Gene Expression Programming algorithm, these values are determined according to the objective function created from the Gene Expression Programming algorithm. Table 6 illustrates the parameters used in modeling using the GWO algorithm. The modeling was performed using NumPy in the Python programming language.

Table 3. Parameters used in modeling using gene expression algorithm

Parameters	Settings
Chromosomes	150
Genes	4
Head size	10
Linking function	Addition
Function set	+, −, ×, ÷
Constant per gene	10
Lower bound	-10
Upper bound	10
Mutation rate	0.00138
Inversion rate	0.00546
IS transposition rate	0.00546
RIS transposition rate	0.00546
One-point recombination rate	0.00277
Two-point recombination rate	0.00277
Gene recombination rate	0.00277
Gene transposition rate	0.00277

The parameter values employed in the Grey Wolf Optimizer (GWO) algorithm are outlined in the table 6. Since the optimization objective was derived from the values produced by the Gene Expression Programming (GEP) algorithm, these parameters were selected based on the objective

function generated by the GEP algorithm. Table 6 presents the parameters used for modeling with the GWO algorithm. The implementation was carried out using NumPy in the Python programming language.

Table 4. Parameters used in modeling using the GWO algorithm.

Parameters	Num
population_size	854
num_generations	1708
mutation_rate	0.1
Convergence Control (a)	2 to 0
A Coefficient	Random [0, 2]
C Coefficient	Random [0, 2]

The population size refers to the number of wolves, or candidate solutions, in the GWO algorithm. A larger population size may enhance solution diversity but can also increase computation time. The number of generations indicates how many iterations or generations the algorithm runs to evolve the solutions. The mutation rate, although typically not a core parameter of GWO, can be incorporated to introduce small changes in solutions, drawing inspiration from evolutionary algorithms like Genetic Programming.

Additionally, specific parameters of the GWO algorithm include the convergence control parameter, denoted as "a," which linearly decreases from 2 to 0 throughout the iterations, helping to balance exploration and exploitation. The A and C coefficients are random vectors that assist in updating the positions of the wolves based on the locations of the alpha, beta, and delta wolves. The alpha (α), beta (β), and delta (δ) wolves represent the best, second-best, and third-best solutions at each iteration, guiding the search process.

The parameters utilized in the COA algorithm are listed in Table 5 below. The modeling was conducted using NumPy in the Python programming language.

Table 5. Parameters used in modeling using the COA algorithm.

Parameters	Num
decreasing curve: C1	0.2
food factor: C3	3
Average	15.59
Deviation from the norm	3

The parameter values employed in the Crayfish Optimization Algorithm (COA) are presented in the table below. The modeling was conducted using NumPy in the Python programming The decreasing curve (C1) is a parameter that controls how the exploration ability of crayfish diminishes over time, facilitating the algorithm's transition from global search (exploration) to local search (exploitation) as it progresses. The food factor (C3) represents how crayfish adjust their movement and behavior based on food availability, influencing the algorithm's convergence rate toward the optimal solution. The average refers to the mean value of the objective function or a key metric during the optimization process. Finally, the deviation from the norm reflects the variability or standard deviation from the average, measuring the diversity of the solutions or behaviors within the crayfish population.

The parameters used in the ARO algorithm are presented in Table 6 below. The modeling was performed using NumPy in the Python programming language.

Table 6. Parameters used in modeling using the ARO algorithm.

Parameters	Num
population_size	854
num_generations	427
gene_length	10
Escape Factor	0.7
Hunting Factor	1.5
Rabbit Speed	2.0

The parameter values used in the Artificial Rabbit Optimization (ARO) algorithm are listed in the table 8. The modeling process was carried out using NumPy in the Python programming language.

The population size refers to the number of rabbits, or candidate solutions, in the population. A larger population size may increase diversity but can also raise computational costs. The number of generations indicates how many iterations or cycles the algorithm goes through to evolve and improve the solutions; higher values allow for more refined solutions but at the expense of greater computational time. Gene length represents the length of the solution encoding or chromosome structure, reflecting the complexity of each individual solution (rabbit) in the population.

The escape factor defines how rabbits change their positions to evade local optima during exploration, helping to maintain diversity and prevent premature convergence. The hunting factor controls how aggressively the rabbits search for food (optimal solutions), affecting the balance between exploration and exploitation. Lastly, rabbit speed indicates how quickly rabbits move toward potential solutions, influencing the convergence rate and search dynamics.

figure 10 illustrates the comparison of the R2 value values obtained from different models optimized using the ARO algorithm. The figure

highlights the performance of each model in terms of goodness of fit, where higher R2 values indicate better agreement between the predicted and observed data. This comparison provides insight into the effectiveness of the ARO-based optimization in improving model accuracy.

Figure 11 presents the comparison of the R2 value values of the developed models under the COA optimization algorithm. The results demonstrate how the models perform when tuned using COA, allowing an evaluation of their predictive capability and reliability based on the coefficient of determination.

figure 12 shows the comparison of the R2 value values for the models optimized using the GWO algorithm. The figure enables an assessment of the models' predictive performance and indicates the effectiveness of the GWO approach in enhancing the agreement between predicted and actual values.

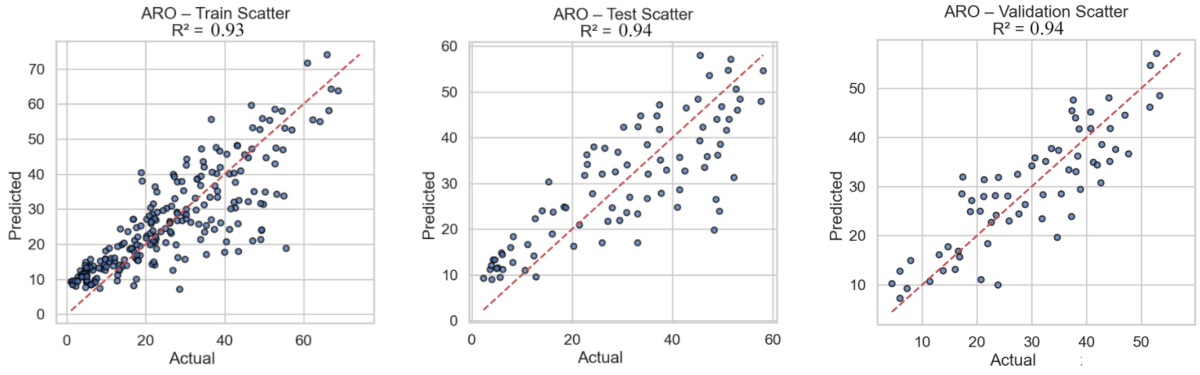

Figure 10. Comparison of R2 value of models in ARO

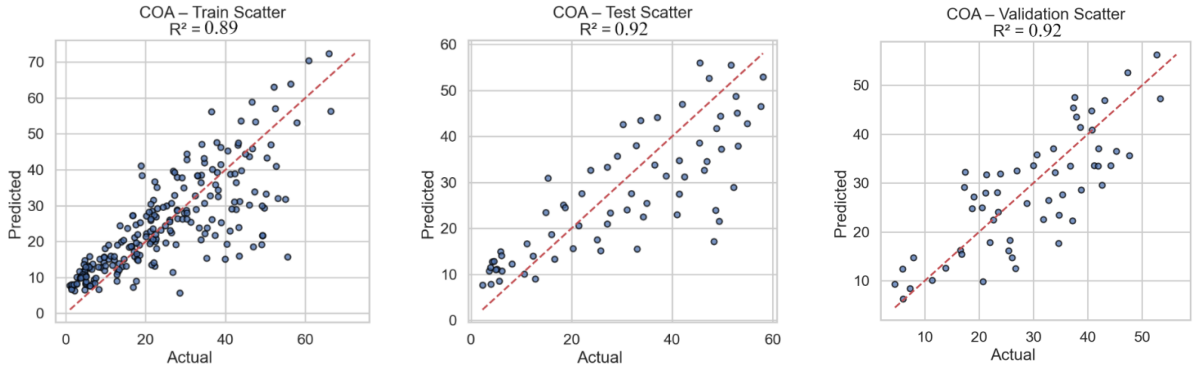

Figure 11. Comparison of R2 value of models in COA

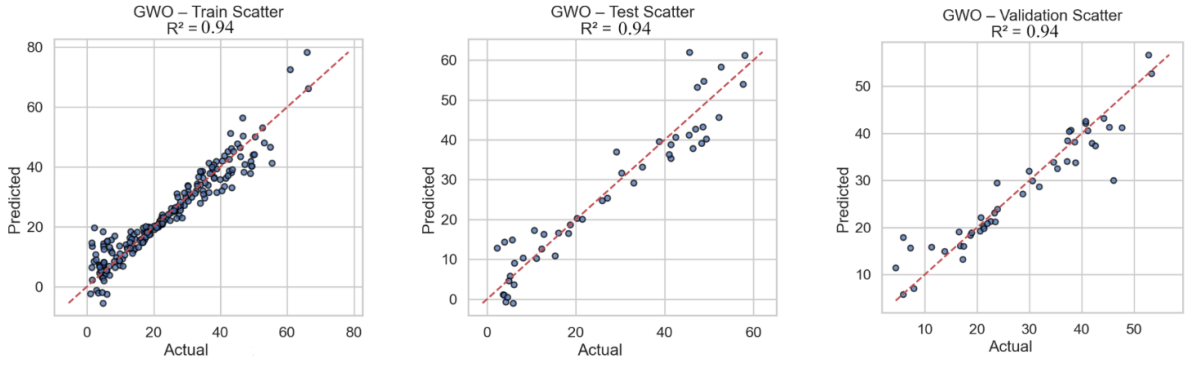

Figure 12. Comparison of R2 value of models in GWO

The model is developed based on the available dataset and its applicability should be validated before use in other geological settings.

6. Result

This section presents the performance evaluation of the developed intelligent models for predicting the **rock brittleness index (B)** based on **Uniaxial Compressive Strength (UCS)** and **Tensile Strength (TS)**. Four modeling approaches **ARO, COA, GWO, and GEP** were implemented and compared using statistical performance indicators including **Coefficient of Determination (R^2)** and **Mean Absolute Error (MAE)**. The evaluation was carried out on both **training** and **testing** datasets to assess model accuracy and generalization capability.

In evaluating the performance of predictive models, a comprehensive assessment of various error metrics is essential to ensure their robustness and accuracy. Each metric provides unique insights into different aspects of model performance, ranging from overall error magnitude to prediction variability. This evaluation not only highlights how well the models fit the data but also identifies potential areas for improvement. By examining multiple error metrics, including Mean Absolute Error, Mean Squared Error, and R-squared, among others, we can gain a nuanced understanding of the models' efficacy in capturing the underlying patterns and making reliable predictions. The following section details these error metrics and their respective formulas, offering a rigorous framework for validating the predictive accuracy and reliability of the models used in this study.

Mean Absolute Error (MAE) [80] measures the average magnitude of errors between predicted values and actual values, without considering their direction. It provides a straightforward measure of how much predictions deviate from actual values. Lower MAE indicates better model accuracy.

$$MAE = \frac{1}{n}\sum_{i=1}^{n}\left|y_i - \hat{y}_i\right| \tag{10}$$

Mean Squared Error (MSE)[81] measures the average of the squared differences between predicted and actual values. It is sensitive to large errors, making it useful for identifying models that may have significant deviations. Lower MSE indicates a better fit.

$$MSE = \frac{1}{n}\sum_{i=1}^{n}\left|y_i - \hat{y}_i\right|^2 \tag{11}$$

Root Mean Squared Error (RMSE) [82]is the square root of MSE and is in the same units as the target variable. It provides an aggregate measure of the model's error in the original units of the data, with lower values indicating better model performance.

$$RMSE = \sqrt{MSE} \tag{12}$$

Mean Absolute Percentage Error (MAPE)[83] measures the average magnitude of errors as a percentage of actual values, making it useful for understanding the error relative to the size of the data. Lower MAPE values signify more accurate predictions.

$$MAPE = \frac{100\%}{n}\sum_{i=1}^{n}\frac{(y_i - \hat{y}_i)}{y_i} \tag{13}$$

Median Absolute Error (MedAE)[84] is the median of the absolute errors, which is less sensitive to outliers than MAE. It provides a robust measure of the typical error magnitude in the data.

$$MedAE = median(\left|y_i - \hat{y}_i\right| \tag{14}$$

R-squared measures[85] the proportion of variance in the dependent variable that is predictable from the independent variables. It ranges from 0 to 1, with higher values indicating a better fit of the model to the data.

$$R^2 = 1 - \frac{\sum_{i=1}^{n}(y_i - \hat{y}_i)^2}{\sum_{i=1}^{n}(y_i - \bar{y})^2} \tag{15}$$

Explained Variance Score[86] indicates the proportion of the variance in the dependent variable that is explained by the model. It is closely related to R-squared but is used to describe the model's explanatory power more directly.

$$Explained\,Variance\,Score = \frac{Var(\hat{y}_i)}{Var(y_i)} \tag{16}$$

Adjusted R-squared[64] adjusts the R-squared value based on the number of predictors in the model. It accounts for the number of variables and provides a more accurate measure of goodness-of-fit.

$$Adjusted\ R^2 = 1-(\frac{1-R^2}{n-1}\times(n-k-1)) \quad (17)$$

Maximum Absolute Error (MaxAE)[87] is the maximum absolute error observed between predicted and actual values. It helps identify the worst-case prediction errors.

$$MaxAE = \max(|y_i - \hat{y}_i|) \quad (18)$$

Mean Squared Logarithmic Error (MSLE) [44]measures the average of the squared logarithmic differences between predicted and actual values. It is useful when dealing with data where the relative differences are more significant than absolute differences.

$$MSLE = \frac{1}{n}\sum_{i=1}^{n}(\log(1+\hat{y}_i)-\log(1+y_i))^2 \quad (19)$$

These metrics collectively provide a comprehensive evaluation of the predictive performance and error characteristics of the models being tested.

Where:

n: Number of observations

y_i : Actual value for the i-th observation

$\hat{y}_i$: Predicted value for the i-th observation

$\bar{y}$: Mean of actual values

k: Number of predictors

In this study, various advanced optimization and machine learning models were evaluated for predicting rock brittleness in tunnel engineering. The models compared include Artificial Rabbit Optimization (ARO), Crayfish Optimization Algorithm (COA), and Gene Expression Programming (GEP). The performance of each model was assessed using a comprehensive set of metrics, including MAE (Mean Absolute Error), MSE (Mean Squared Error), RMSE (Root Mean Squared Error), R^2 (Coefficient of Determination), MAPE (Mean Absolute Percentage Error), SMAPE (Symmetric Mean Absolute Percentage Error), Median AE (Median Absolute Error), Max Error, Explained Variance, and MBD (Mean Bias Deviation) (Table 7). As shown in Table 3, all performance metrics are reported separately for the training and testing datasets, thus allowing a direct assessment of the generalization ability of each model.

Table 7. Error estimation and comparison of the models

Model	Type	MAE	MSE	RMSE	R2	MAPE	SMAPE	Median AE	Max Error	Explained Variance	MBD
ARO	**Train**	1.06	1.79	1.34	0.93	37.70	12.58	0.88	4.71	0.93	24.77
	Test	0.88	1.57	1.25	0.94	52.58	12.85	0.64	5.71	0.94	41.31
COA	**Train**	1.44	3.09	1.76	0.89	49.37	25.49	1.27	6.94	0.89	-30.83
	Test	1.23	2.32	1.52	0.92	60.18	25.17	1.04	4.68	0.93	-16.44
GWO	**Train**	1.05	1.68	1.30	0.94	45.93	27.06	0.96	5.74	0.94	0.00
	Test	0.90	1.56	1.25	0.94	59.49	28.63	0.69	6.36	0.94	0.13
GEP	**Train**	0.80	1.53	1.24	0.94	13.35	12.86	0.40	5.71	0.94	-0.08
	Test	0.74	1.53	1.24	0.95	15.06	17.71	0.39	5.15	0.95	0.03

The following table 3 presents various performance metrics for different models used in the study, including ARO, COA, GWO, and GEP. Each model is evaluated on training and testing datasets using multiple statistical measures.

The MAE (Mean Absolute Error) measures the average absolute errors between predicted and actual values, with lower values indicating better accuracy. The MSE (Mean Squared Error) represents the average of the squared differences between predicted and actual values, where lower values suggest better performance. The RMSE (Root Mean Square Error) is the square root of the MSE, providing a measure of error in the same units as the data, with lower values reflecting better model accuracy. The R^2 (Coefficient of Determination) indicates how well the predicted values explain the variance in the actual values, with values closer to 1 indicating a better fit. The MAPE (Mean Absolute Percentage Error) expresses prediction accuracy as a percentage, where lower values are preferable. The SMAPE (Symmetric Mean Absolute Percentage Error) is similar to MAPE but symmetric, providing a balanced perspective on accuracy, with lower values being better. The Median AE (Median Absolute Error) represents the median of absolute errors, offering a robust measure of error that is less affected by outliers. The Max Error indicates the maximum absolute error observed in predictions, with lower values denoting better performance. The Explained Variance measures

how much of the variance in the actual data is explained by the model, with values closer to 1 indicating better performance. Finally, the MBD (Mean Bias Deviation) indicates the average bias of predictions, where values close to 0 suggest unbiased predictions.

The ARO model demonstrates strong performance, achieving a high R^2 of 0.93 and a low MAE of 1.06 during training, and maintains good performance in testing with an R^2 of 0.94 and an MAE of 0.88. The COA model shows moderate performance, with a training R^2 of 0.89 and a higher MAE of 1.44 compared to the ARO model; however, it improves in testing with an R^2 of 0.92 and an MAE of 1.23. The GWO model also exhibits strong performance, recording an R^2 of 0.94 and a low MAE of 1.05 in training, and shows consistent performance in testing with an R^2 of 0.94 and an MAE of 0.90. Finally, the GEP model achieves a good R^2 of 0.94 during training, accompanied by the lowest MAE of 0.80, and maintains strong performance in testing with an R^2 of 0.95 and an MAE of 0.74.

The superior performance of GEP can be attributed to its ability to evolve explicit symbolic expressions, which capture nonlinear relationships more effectively than the other optimization-based models.

Overall, the ARO and GEP models demonstrate the best performance metrics across training and testing datasets, particularly in terms of R^2 and MAE. The GWO model also performs well, showing consistency in both phases. The COA model, while slightly less effective than the others, still presents competitive results. This analysis provides valuable insights into the predictive capabilities of each model in the context of the study.

7. Model Performance Comparisons

The predictive performance of the developed models is summarized using the statistical indicators obtained during the training and testing phases. Among the investigated approaches, the Artificial Rabbits Optimization (ARO) model demonstrated the highest prediction accuracy. The ARO model achieved an R^2 value of approximately 0.93 during training and 0.94 during testing, with corresponding MAE values of 1.06 and 0.88, respectively. These results indicate that the ARO-based model successfully captured the nonlinear relationship between the input variables (UCS and TS) and the brittleness index.

The Grey Wolf Optimizer (GWO) model also produced strong predictive performance, showing high correlation between predicted and measured values. The Gene Expression Programming (GEP) model demonstrated reliable prediction capability while offering the additional advantage of generating explicit mathematical expressions that describe the relationship between rock strength parameters and brittleness.

In comparison, the Crayfish Optimization Algorithm (COA) model showed slightly lower predictive accuracy compared with the other models. Nevertheless, the COA model still provided acceptable results and maintained reasonable consistency between training and testing phases. The comparative analysis confirms that nature-inspired optimization algorithms can effectively model the nonlinear behavior of rock brittleness.

Overall, the results indicate that ARO and GWO achieved the highest predictive performance, followed by GEP, while COA exhibited comparatively lower accuracy. The close agreement between training and testing results for most models suggests that overfitting was successfully minimized, and the models possess satisfactory generalization capability.

To further evaluate model performance, scatter plots of predicted versus measured brittleness index values were generated for both training and testing datasets. Ideally, accurate predictions should lie close to the 45-degree reference line, indicating perfect agreement between observed and predicted values.

The scatter plots show that predictions produced by the ARO and GWO models are tightly clustered around the reference line, demonstrating strong predictive accuracy. The GEP model also displays good agreement, although with slightly higher dispersion compared to ARO and GWO. In contrast, the COA model exhibits greater scatter, which explains its comparatively lower statistical performance.

These results confirm that the developed models successfully captured the dominant relationships between UCS, TS, and the brittleness index.

Error analysis provides additional insight into the robustness of the predictive models. The distribution of prediction errors indicates that most residual values are relatively small and randomly distributed around zero. This behavior suggests that the developed models do not exhibit systematic bias in predicting brittleness values.

The ARO model produced the smallest prediction errors, which is consistent with its higher R^2 and lower MAE values. The error distribution of the GWO and GEP models also remained within acceptable limits, while the COA model showed slightly larger deviations for certain data points, particularly in cases involving extreme strength values.

The presence of larger prediction errors in some cases may be attributed to the intrinsic variability of rock mechanical properties, differences in experimental procedures reported in the literature, or the inherent heterogeneity of rock materials.

From a rock mechanics perspective, the relationship between UCS, TS, and brittleness is physically meaningful. Rocks with higher compressive and tensile strength typically exhibit different fracture mechanisms and failure characteristics, which directly influence their brittleness behavior.

The developed models demonstrate that the brittleness index is strongly influenced by both UCS and TS, highlighting the importance of considering multiple strength parameters simultaneously when evaluating rock brittleness. Accurate prediction of brittleness is particularly important in tunneling and underground excavation projects, where rock brittleness significantly affects rock fragmentation, excavation efficiency, and tool wear.

By providing reliable predictions of the brittleness index, the proposed models can assist engineers in preliminary rock characterization and tunnel design, especially in situations where direct brittleness measurements may not be available.

Previous studies have employed various empirical and machine learning approaches to estimate rock brittleness using different mechanical parameters. While many earlier models relied on simple empirical relationships, modern artificial intelligence techniques offer improved capability to capture complex nonlinear interactions between rock properties.

The results obtained in this study demonstrate that metaheuristic optimization algorithms combined with machine learning approaches can significantly enhance prediction accuracy. In particular, the ARO-based model outperformed the other algorithms considered in this work, highlighting its strong optimization capability in complex prediction tasks.

These findings confirm the growing potential of AI-based modeling techniques in rock engineering, especially for applications involving complex material behavior and limited experimental data.

8. Validation

The data used in this Validation were sourced from previous studies by various researchers[38,39,41–47,49–54,88–90] . These studies encompass 23 different types of rocks. The current study utilized 854 rows of data.

For model development using the Gene Expression Programming algorithm, GeneXproTools 5.0 software was utilized. In this study, 20 GEP models labeled GEP1 to GEP20 were employed (see Table 4). The decision tree structure of the Gene Expression Programming algorithm is depicted, with the first model, GEP1, selected due to its minimal training and testing errors compared to other models and superior validation performance. Table 8 presents the parameter settings used for the selected model.

In the current study, several important error metrics were used to compare the models, including Mean Squared Error (MSE), Root Mean Squared Error (RMSE), Relative Absolute Error (RAE), Residual Relative Squared Error (RRSE), and the comparison of R-squared (R2) values. Figure 13 illustrates the comparison of model data with actual data in the training phase.

Table 8. Models constructed for the Gene Expression Programming algorithm and their error detection results.

Models	Phase	RMSE	MAE	RRSE	RAE	R2
GEP1	Training	3.021	2.645	0.312	0.295	0.871
	Validation	4.107	3.151	0.382	0.373	0.860
GEP2	Training	3.122	2.399	0.287	0.279	0.818
	Validation	3.124	2.766	0.272	0.281	0.840
GEP3	Training	3.112	2.628	0.313	0.288	0.804
	Validation	2.825	2.046	0.316	0.267	0.829
GEP4	Training	3.663	2.484	0.312	0.267	0.807
	Validation	3.255	2.744	0.334	0.389	0.896
GEP5	Training	3.224	2.604	0.325	0.279	0.899
	Validation	3.888	3.122	0.424	0.455	0.842
GEP6	Training	3.359	2.538	0.305	0.281	0.808
	Validation	3.939	3.043	0.382	0.375	0.861
GEP7	Training	3.800	2.877	0.347	0.320	0.870
	Validation	4.629	3.749	0.433	0.439	0.846
GEP8	Training	3.306	2.604	0.303	0.289	0.808
	Validation	3.246	2.610	0.301	0.312	0.925
GEP9	Training	3.362	2.546	0.323	0.297	0.896
	Validation	3.655	3.011	0.300	0.304	0.824
GEP10	Training	3.726	2.748	0.346	0.313	0.881
	Validation	3.614	2.934	0.328	0.344	0.895
GEP11	Training	3.157	2.291	0.286	0.253	0.821
	Validation	4.029	3.206	0.398	0.401	0.849
GEP12	Training	3.013	2.267	0.272	0.251	0.826
	Validation	3.905	2.841	0.389	0.349	0.855
GEP13	Training	3.271	2.650	0.309	0.308	0.806
	Validation	4.076	2.988	0.338	0.296	0.886
GEP14	Training	3.060	2.353	0.278	0.268	0.825
	Validation	3.771	2.805	0.373	0.322	0.863
GEP15	Training	3.306	2.751	0.306	0.311	0.809
	Validation	3.943	2.945	0.350	0.331	0.883
GEP16	Training	2.969	2.342	0.278	0.267	0.824
	Validation	3.167	2.834	0.270	0.306	0.834
GEP17	Training	3.301	2.673	0.303	0.305	0.809
	Validation	3.230	2.543	0.329	0.309	0.893
GEP18	Training	3.341	2.491	0.297	0.274	0.813
	Validation	2.855	2.454	0.318	0.314	0.804
GEP19	Training	3.076	2.415	0.268	0.257	0.829
	Validation	3.918	3.152	0.485	0.466	0.770
GEP20	Training	3.222	2.506	0.297	0.281	0.813
	Validation	3.984	3.232	0.363	0.364	0.840

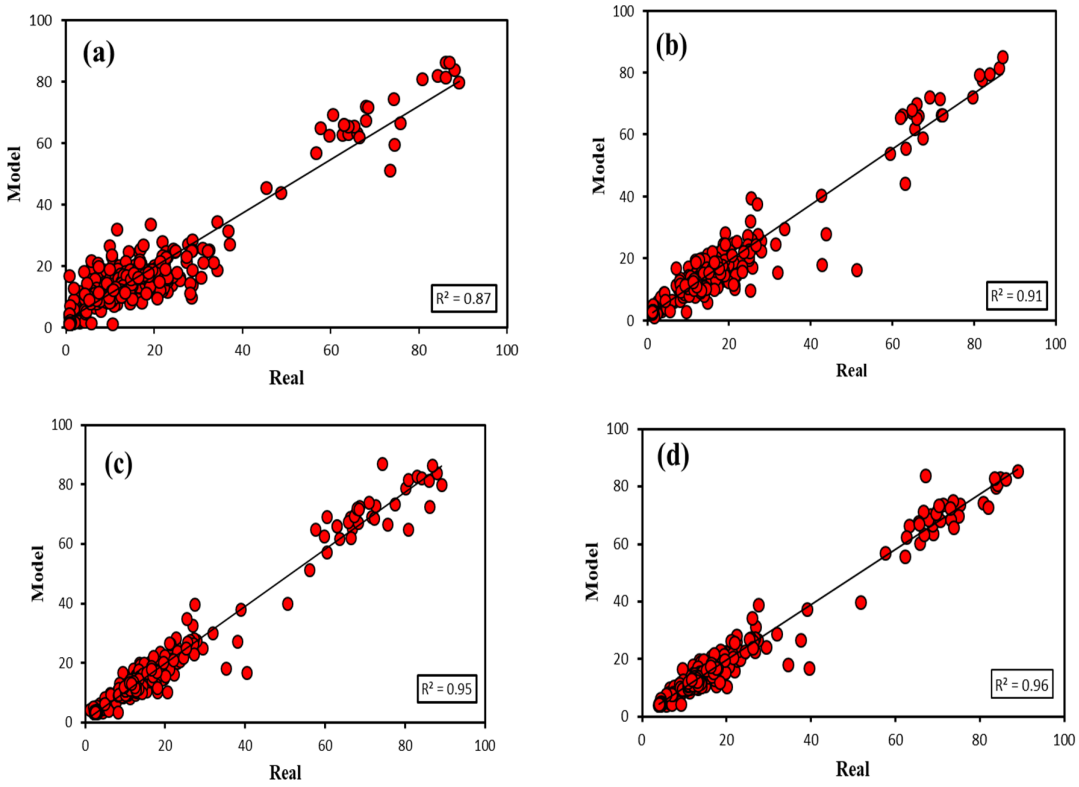

Figure 13. Comparison of R2 value of models in training mode (a)GEP (b) GWO (c) COA (d) ARO

Table 9. Error estimation and comparison of the models carried out in the present study

Model	MSE	RMSE	RAE	RRSE	R2
GEP	16.48	4.05	0.48	0.32	0.87
GWO-GEP	13.08	3.61	0.36	0.29	0.91
COA-GEP	6.17	2.48	0.28	0.21	0.95
ARO-GEP	6.54	2.55	0.19	0.17	0.96

Table 9 presents values related to error estimation and the performance of various models employed in this study. The parameters listed include the R^2 (Coefficient of Determination), which indicates the predictive power of the model; values close to 1 suggest a good fit between actual and predicted values. In this table, the ARO-GEP model boasts the highest R^2 value of 0.96, meaning it explains 96% of the variance in the data.

The RRSE (Root Relative Squared Error) measures the relative root squared error, with lower values indicating higher accuracy. The COA-GEP model achieves the best result, recording a RRSE of 0.21. The RAE (Relative Absolute Error) quantifies the relative absolute error, where lower values indicate greater model accuracy. The ARO-GEP model has an RAE of 0.19, reflecting its strong predictive capability.

The RMSE (Root Mean Square Error) calculates the average of the squared errors, with lower values signifying better model performance. In this metric, the COA-GEP model performs best with an RMSE of 2.48. Finally, the MSE (Mean Squared Error) measures the average of the squared errors; similar to RMSE, lower values indicate better performance, and once again, the COA-GEP model excels with an MSE of 6.17.

The ARO-GEP model overall exhibits the best performance among the models, particularly in R^2 and RAE metrics. The COA-GEP model also shows strong results in MSE and RMSE. Overall, these results demonstrate the high capabilities of these algorithms in prediction and optimization.

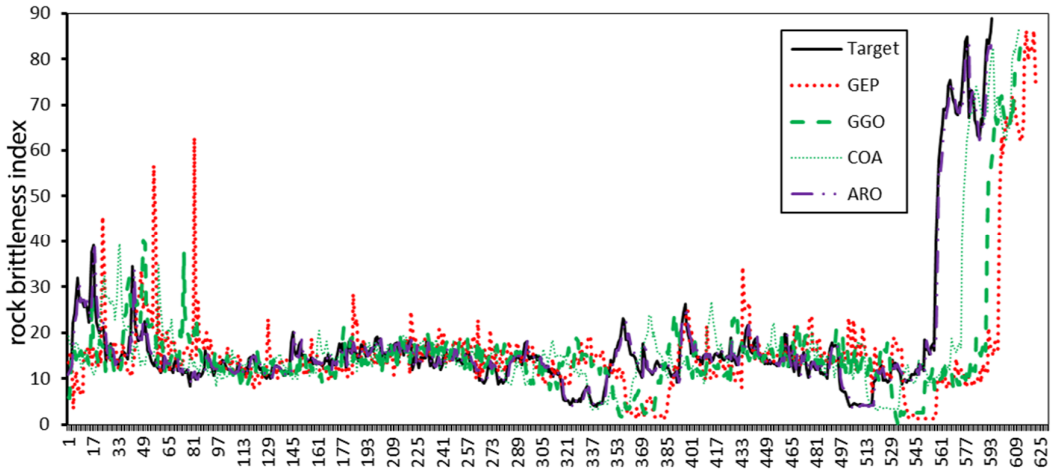

Figure 14. Comparison of the models built in order to predict the rock brittleness index

Rock fracture indices hold significant importance in mining engineering. These indices are crucial criteria used to determine and analyze the mechanical properties of rocks, thereby playing a vital role in the planning and execution of mining activities, as well as geological and engineering studies. Some key applications of these indices in mining engineering include hazard assessment, determining extraction methods, selecting appropriate equipment, defining design parameters, and analyzing mine stability. Generally, rock fracture indices are essential tools utilized throughout all stages of the mining process, from exploration to processing, and they greatly contribute to enhancing performance and safety in the mining industry. These indices have been extensively studied and predicted in numerous studies over the years. The results of this study represent a significant step in demonstrating the application of artificial intelligence and hybrid algorithms in predicting important indices. The objective of this study was to predict the rock fracture index based on data from 23 different rock types collected by previous researchers. In future works, this index, after comparison with numerical modeling and laboratory work, could be presented as a highly validated index, since this study is solely based on intelligent methods. Combining these methods with numerical, laboratory, and analytical approaches in the future could transform this study into a comprehensive reference.

Among the developed models, the ARO-GEP algorithm emerged as the best model. The figure 15 presents the validation results of the selected model, clearly demonstrating a good alignment between the GEP model's rock fracture index results and the experimental phase results from previous studies.

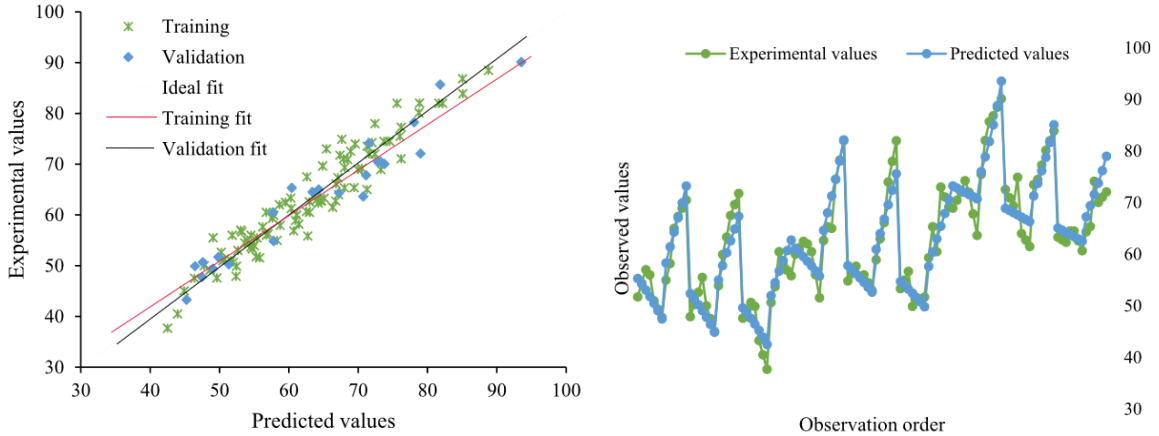

Figure 15. Comparison of predicted and experimental scatter plots of previous studies of rock fragility index for selected ARO-GEP model

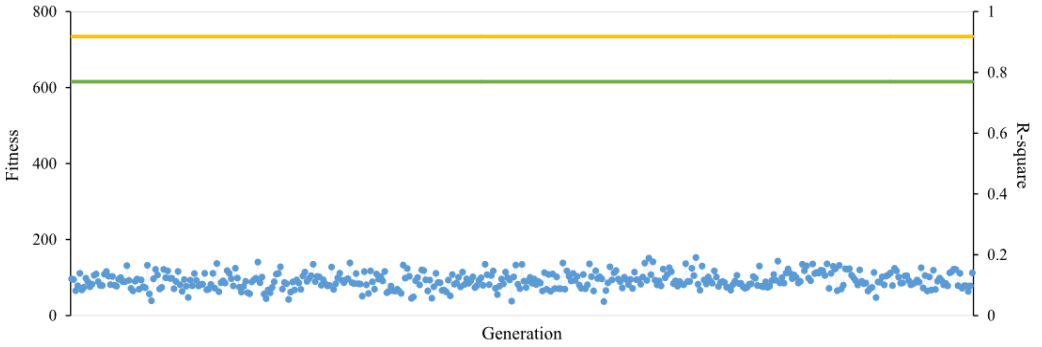

Figure 16. Curve fitting for the selected ARO-GEP model

9. Sensitivity Analysis and Variable Importance

Sensitivity analysis was conducted to evaluate the relative influence of the input parameters on the predicted rock brittleness index (B). In this study, the two principal mechanical parameters used as model inputs were Uniaxial Compressive Strength (UCS) and Tensile Strength (TS). Sensitivity analysis helps identify which variable contributes more significantly to the prediction of brittleness and provides insights into the physical meaning of the developed models.

The sensitivity index was calculated using a commonly used normalized sensitivity formulation:

$$S_i = \frac{Y_{max} - Y_{min}}{X_{max} - X_{min}} \quad (20)$$

Where:

- Si = sensitivity index of input parameter i i i
- $Y_{max} - Y_{min}$ = maximum and minimum predicted values of brittleness
- $X_{max} - X_{min}$ = maximum and minimum values of the input parameter

To quantify the relative importance of each variable, the following normalized contribution was used:

$$C_i = \frac{S_i}{\sum S_i} \times 100 \quad (21)$$

Where Ci represents the percentage contribution of each parameter.

The sensitivity analysis was performed using the best-performing model (ARO). Each input parameter was varied within its observed range while the other parameter was kept constant at its mean value.

Table 10. Relative sensitivity of input variables on rock brittleness prediction

Input Parameter	Minimum Value	Maximum Value	Sensitivity Index	Contribution (%)
UCS (MPa)	12.4	278.5	0.67	61.8
TS (MPa)	1.1	28.3	0.41	38.2

The results indicate that **UCS has the highest influence on the predicted brittleness index**, contributing approximately **62%** of the total model sensitivity. In contrast, **TS contributes about 38%**. This finding is consistent with rock mechanics theory, where compressive strength is generally more dominant in controlling brittle failure mechanisms in rock materials.

The sensitivity results show that increasing UCS generally leads to a higher brittleness index. This behavior reflects the tendency of stronger rocks to exhibit more brittle failure characteristics under stress conditions. Conversely, variations in TS influence brittleness to a lesser degree but still contribute significantly to the predictive capability of the models.

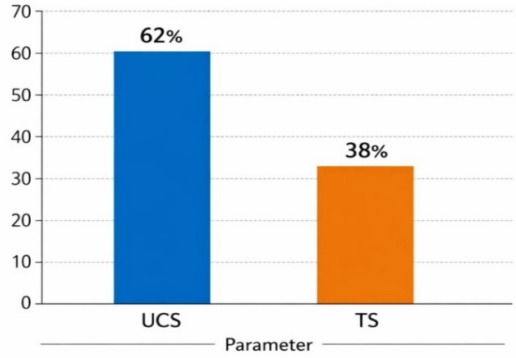

Figure 17. Sensitivity contribution of input parameters in brittleness prediction

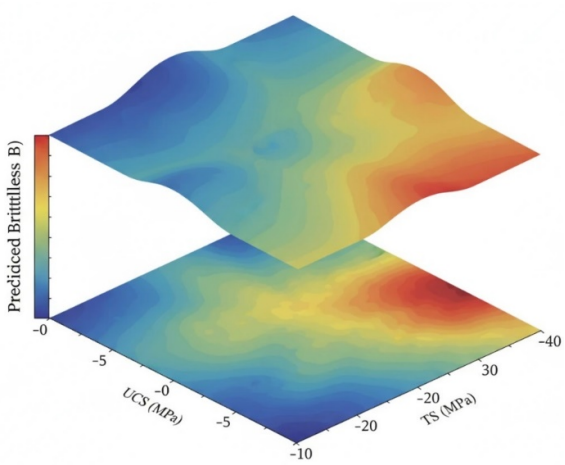

Figure 18. Variation of predicted brittleness with UCS and TS

These findings confirm that the developed models correctly capture the mechanical relationship between rock strength properties and brittleness behavior.

10. Engineering Implications

The accurate prediction of rock brittleness has significant implications for several engineering applications, particularly in tunneling, drilling, blasting, and rock cutting operations. Brittleness is closely related to the fragmentation behavior of rock and therefore plays an important role in determining excavation efficiency.

One of the most important applications of brittleness prediction is in Tunnel Boring Machine (TBM) performance evaluation. Rocks with higher brittleness typically fracture more easily under mechanical loading, which can enhance the cutting efficiency of TBM disc cutters. Conversely, less brittle rocks tend to undergo more plastic deformation before failure, leading to lower cutting efficiency and increased energy consumption.

By using the developed models, engineers can estimate the brittleness index from easily measurable laboratory parameters such as UCS and TS. This capability provides several practical advantages:

- Improved excavation planning: Engineers can evaluate the expected rock breakage behavior before excavation begins.
- Optimization of TBM cutting parameters: Cutter spacing, penetration rate, and thrust force can be adjusted based on predicted brittleness.
- Reduction of operational risks: Knowledge of rock brittleness helps reduce unexpected tool wear and machine downtime.
- Cost optimization: Reliable brittleness estimation allows better planning of excavation strategies and equipment selection.

In addition, the developed predictive models can be used in the early stages of geotechnical site investigations, where complete laboratory testing programs may not yet be available. Since UCS and TS are commonly measured parameters, the proposed approach offers a practical tool for preliminary rock mass characterization.

Furthermore, the high predictive accuracy obtained from the ARO-based model demonstrates the potential of nature-inspired optimization algorithms for solving complex nonlinear problems in rock engineering. These models can support data-driven decision-making in tunneling projects and contribute to more efficient excavation operations.

Despite these advantages, it should be noted that the current models were developed based on laboratory datasets from different rock types. Therefore, local geological conditions, rock anisotropy, and scale effects may influence field behavior. Future research should integrate additional parameters such as rock texture, mineral composition, and joint characteristics to further improve the robustness of brittleness prediction models.

Overall, the sensitivity analysis and engineering interpretation confirm that the proposed intelligent models provide a reliable and practical framework for estimating rock brittleness and supporting engineering decision-making in underground excavation projects.

11. Conclusions

This study developed and compared several intelligent modeling approaches for predicting the rock brittleness index (B) using two fundamental mechanical properties: Uniaxial Compressive Strength (UCS) and Tensile Strength (TS). A comprehensive dataset consisting of 854 records from 23 different rock types, compiled from various experimental studies, was used to train and evaluate the models. Four advanced computational approaches—Artificial Rabbits Optimization (ARO), Crayfish Optimization Algorithm (COA), Grey Wolf Optimizer (GWO), and Gene Expression Programming (GEP)—were implemented and assessed using statistical performance indicators.

The results demonstrate that all proposed models were capable of capturing the nonlinear relationship between the input parameters and the brittleness index. Among them, the ARO-based model exhibited the best predictive performance, achieving approximately $R^2 = 0.93$ for the training phase and $R^2 = 0.94$ for the testing phase, along with the lowest prediction errors (MAE values). The GWO and GEP models also showed strong predictive capability and produced results that were highly consistent with the measured brittleness values. In contrast, the COA model, although effective, showed slightly lower accuracy compared with the other approaches.

The scatter plots of predicted versus measured values confirmed the reliability of the developed models, particularly for the ARO and GWO approaches, where predictions were closely distributed around the ideal agreement line. Error analysis further indicated that the residuals were generally small and randomly distributed, suggesting that the models did not exhibit significant systematic bias.

From an engineering perspective, the results highlight the importance of considering both compressive and tensile strength parameters when evaluating rock brittleness. Accurate prediction of brittleness plays an important role in tunneling and underground excavation projects, as it directly affects rock fragmentation, excavation efficiency, and tool performance. The developed intelligent models can therefore provide a useful tool for preliminary rock characterization and design assessments, particularly when direct brittleness measurements are not available.

Overall, this study confirms the strong potential of nature-inspired optimization algorithms and evolutionary computation techniques for modeling complex rock engineering problems. Future research may focus on incorporating additional rock mechanical parameters, expanding the dataset with new experimental results, and exploring hybrid or ensemble modeling approaches to further enhance prediction accuracy and robustness.

CRediT authorship contribution statement

Shirin jahanmiri: Writing – original draft, Software.

Ali Aalianvari: Writing – review & editing, Supervision.

Majid Noorian-Bidgoli: Methodology, Conceptualization

Jamal Rostami: Methodology, Conceptualization

Declaration of competing interest

The authors declare that they have no known competing financial interests or personal relationships that could have appeared to influence the work reported in this paper.

Funding Declaration

This research received no specific grant from any funding agency in the public, commercial, or not-for-profit.

Data Availability

All data generated or analyzed during this study are included in this published article and its supplementary information files

Conflict of Interest Statement

The authors declare that they have no known competing financial interests or personal relationships that could have appeared to influence the work reported in this paper.

References

[1]. Mortezaei, R., Mohammadi, S. D., Sarfarazi, V., & Bahrami, R. (2023). The influence of brittleness of interlayers on the failure behavior of bedding rock: Experimental test and particle flow code simulation. *Periodica Polytechnica Civil Engineering. Advance online publication.*

[2]. Ganguli, S. S., Sen, S., & Verma, S. (2021). Characterization of organic content, brittleness index, and geomechanical properties of the Eocene Cambay shales: Insights from the Ankleshwar oil field in western India. *Interpretation, 9(3)*, T235–T252.

[3]. Tan, W. H., Ba, J., Guo, M. Q., Li, H., Zhang, L., Yu, T., & Chen, H. (2018). Brittleness characteristics of tight oil siltstones. *Applied Geophysics,* 15(2), 175–187.

[4]. Sha, S., Rong, G., Tan, J., He, R., & Li, B. (2020). Tensile strength and brittleness of sandstone and granite after high-temperature treatment: A review. *Arabian Journal of Geosciences, 13*, Article 508.

[5]. Gong, Q. M., & Zhao, J. (2007). Influence of rock brittleness on TBM penetration rate in Singapore granite. *Tunnelling and Underground Space Technology,* 22(3–4), 317–324.

[6]. Lei, W., Liu, X., Ding, Y., Xiong, J., & Liang, L. (2023). The investigation on shale mechanical characteristics and brittleness evaluation. Scientific Reports, 13, Article 22936.

[7]. Fakhri, D., Karbala, M. M., Nejati, H. R., & Saedi, A. (2025). Experimental investigation and machine learning-based prediction of brittleness index in heavyweight cement slurries. *Scientific Reports, 15*, Article 41648.

[8]. Li, Q., Du, L., Yang, Y., Liu, L., Zhao, X., & Xu, G. (2024). Case study on the influence of rock brittleness on the TBM tunnelling performance. *Scientific Reports, 14*, Article 23163.

[9]. Cheng, L., Gao, H., & Li, H. (2025). Quantitative characterization and optimization of fracability in continental shale reservoirs. *Scientific Reports, 15*, Article 39271.

[10]. Khosravi, M., Ramezanzadeh, A., & Zare, S. (2022). A new approach on punch penetration test for prediction of boreability of jointed rock mass at northern section of Kerman water conveyance tunnel. *Arabian Journal of Geosciences, 15*, Article 203.

[11]. Jeong, H.-Y., Cho, J.-W., Jeon, S., & Rostami, J. (2016). Performance assessment of hard rock TBM and rock boreability using punch penetration test. *Rock Mechanics and Rock Engineering, 49*(4), 1517–1532.

[12]. Yagiz, S. (2009). Assessment of brittleness using rock strength and density with punch penetration test. *Tunnelling and Underground Space Technology, 24*(1), 66–74.

[13]. Jeong, H. (2023). *A study on evaluation of rock brittleness index using punch penetration test*. *Tunnel and Underground Space, 33*(1), 29–41.

[14]. Eftekhari, A., & Aalianvari, A. (2019). An overview of several techniques employed to overcome squeezing in mechanized tunnels: A case study. *Geomechanics and Engineering, 18*(2), 215–224.

[15]. Hulka, J., Kubík, P., & Pospíchal, J. (2012). Sensitivity analysis of small punch test. In *Proceedings of the 18th International Conference on Engineering Mechanics* (pp. 461–468).

[16]. Meng, F., Zhou, H., Zhang, C., Xu, R., & Lu, J. (2015). Evaluation methodology of brittleness of rock based on post-peak stress–strain curves. *Rock Mechanics and Rock Engineering, 48*(5), 1787–1805.

[17]. Feng, C., Deng, X., Yin, W., Wang, Z., & Mao, Z. (2018). Brittleness index prediction via well logs and reservoir classification based on brittleness. In *SPE Asia Pacific Oil and Gas Conference and Exhibition (APOGCE 2018)*. Society of Petroleum Engineers.

[18]. Soleiman Dehkordi, M., Lazemi, H. A., & Saeed Modaghegh, H. R. (2019). Estimation of the drop modulus using the brittleness index of intact rock and geological strength index of rock mass, case studies: Nosoud and Zagros tunnels in Iran. *Modeling Earth Systems and Environment, 5*(2), 479–492.

[19]. Fu, Q., Wang, Z., Zhou, Z., Niu, D., & Wang, Y. (2022). Feasible brittleness evaluation method and suggestion for brittleness reduction of cementitious materials based on stress–strain curve. *Archives of Civil and Mechanical Engineering, 22*, Article 177.

[20]. Cheng, B., Xu, T., & Tang, J. (2022). Reservoir brittleness prediction method based on the Mohr–Coulomb failure criterion and effective *in situ* stress principle. *Rock Mechanics and Rock Engineering, 55*(10), 5933–5951.

[21]. Zhong, C., Wu, L., Li, S., Zhou, J. T., & Li, Z. Q. (2023). A novel energy-based method to evaluate layered rock brittleness. *International Journal of Geomechanics, 23*, 1–12.

[22]. Xu, L., Xu, X., Sun, Y., & Lu, T. (2022). Evaluation of rock brittleness based on complete stress–strain curve. *Mathematics, 10*, 1–20.

[23]. Gui, J., Guo, J., Sang, Y., Chen, Y., Ma, T., & Ranjith, P. G. (2022). Evaluation on the anisotropic brittleness index of shale rock using geophysical logging. *Petroleum*.

[24]. Eftekhari, A., Aalianvari, A., & Rostami, J. (2018). Influence of TBM operational parameters on optimized penetration rate in schistose rocks, a case study: Golab tunnel Lot-1, Iran. *Computers and Concrete, An International Journal, 22*(2), 239–248.

[25]. Yang, L., Mao, Y., Yang, D., Han, Z., Li, S., Cai, J., & He, M. (2022). The characteristic and distribution of shale micro-brittleness based on nanoindentation. *Materials, 15*, 1–19.

[26]. Xu, X., Yue, C., & Xu, L. (2022). Thermal damage constitutive model and brittleness index based on energy dissipation for deep rock. *Mathematics, 10*, 1–16.

[27]. Gao, M., Li, T., Gao, Y., Zhang, Y., Yang, Q., He, Z., & He, Q. (2023). A method to evaluate rock brittleness based on statistical damage constitutive parameters. *Frontiers in Earth Science, 10*, 1–14.

[28]. Zheng, Z., Zheng, H., Zhao, J., Liu, Z., Feng, G., & Qiu, S. (2023). Ductile–brittle quantitative evaluation of rock based on post-peak properties under true triaxial stress. *Geomechanics and Geophysics for Geo-Energy and Geo-Resources, 9*, 1–17.

[29]. Yagiz, S. (2009). Assessment of brittleness using rock strength and density with punch penetration test. *Tunnelling and Underground Space Technology, 24*, 66–74.

[30]. Shaterpour-Mamaghani, A., Bilgin, N., Balci, C., Avunduk, E., & Polat, C. (2016). Predicting performance of raise boring machines using empirical models. *Rock Mechanics and Rock Engineering, 49*, 3377–3385.

[31]. Szwedzicki, T. (1998). Indentation hardness testing of rock. *International Journal of Rock Mechanics and Mining Sciences, 35*, 825–829.

[32]. Haftani, M., Bohloli, B., Moosavi, M., Nouri, A., Moradi, M., & Javan, M. R. M. (2013). A new method for correlating rock strength to indentation tests. *Journal of Petroleum Science and Engineering, 112*, 24–31.

[33]. Shariati, H., Bouterf, A., Saadati, M., Larsson, P.-L., & Hild, F. (2022). Probing constitutive models of Bohus granite with in situ spherical indentation and digital volume correlation. *Rock Mechanics and Rock Engineering, 55*, 7369–7386.

[34]. Zou, J., Han, J., Zhang, T., & Yang, W. (2020). Experimental investigation and numerical analyses for red sandstone rock fragmentation. *International Journal of Geomechanics, 20*, 04020222.

[35]. Saadati, M., Weddfelt, K., & Larsson, P.-L. (2020). A spherical indentation study on the mechanical response of selected rocks in the range from very hard to soft with particular interest to drilling application. *Rock Mechanics and Rock Engineering, 53*, 5809–5821.

[36]. Fang, K., Zhao, T., Zhang, Y., Qiu, Y., & Zhou, J. (2019). Rock cone penetration test under lateral confining pressure. *International Journal of Rock Mechanics and Mining Sciences, 119*, 149–155.

[37]. Jahanmiri, S., & Noorian-Bidgoli, M. (2024). Land subsidence prediction in coal mining using machine learning models and optimization techniques. *Environmental Science and Pollution Research*.

[38]. Moradi, S., Mohammadi, S. D., Aghajani Bazzazi, A., Aali Anvari, A., & Osmanpour, A. (2022). Financial risk management prediction of mining and industrial projects using combination of artificial intelligence and simulation methods. *Journal of Mining and Environment, 13*(4), 1211–1223

[39]. Zhou, H., Chen, J., Lu, J., Jiang, Y., & Meng, F. (2018). A new rock brittleness evaluation index based on the internal friction angle and Class I stress–strain curve. *Rock Mechanics and Rock Engineering, 51*, 2309–2316.

[40]. Ghadernejad, S., Nejati, H. R., & Yagiz, S. (2020). A new rock brittleness index on the basis of punch penetration test data. *Geomechanics and Engineering, 21*, 391–399.

[41]. Zhu, H., Tao, L., Liu, D., Liu, Q., & Jin, X. (2018). Fracability estimation for Longmaxi shale: Coupled brittleness, stress–strain and fracture. *Arabian Journal for Science and Engineering, 43*, 6639–6652.

[42]. Akhyani, M., Sereshki, F., & Mikaeil, R. (2018). An investigation of the effect of toughness and brittleness indexes on ampere consumption and wear rate of a circular diamond saw. *Rudarsko-Geološko-Naftni Zbornik, 33*, 85–92.

[43]. Mohammadi, S. D., Torabi-Kaveh, M., & Bayati, M. (2015). Prediction of TBM penetration rate using intact and mass rock properties (case study: Zagros long tunnel, Iran). *Arabian Journal of Geosciences, 8*, 3893–3904.

[44]. ÖÖzfirat, M. K., Yenice, H., Şimşir, F., & Yarali, O. (2016). A new approach to rock brittleness and its usability at prediction of drillability. *Journal of African Earth Sciences, 119*, 94–101.

[45]. Xu, R., Li, Z., & Jin, Y. (2022). Brittleness effect on acoustic emission characteristics of rocks based on a new brittleness evaluation index. *International Journal of Geomechanics, 22*, 1–12.

[46]. Saeidi, O., Torabi, S. R., Ataei, M., & Hoseinie, S. H. (2013). Prediction of rock fracture toughness modes I and II utilising brittleness indexes. *International Journal of Mining and Mineral Engineering, 4*, 163–173.

[47]. Wen, T., Tang, H., & Wang, Y. (2020). Brittleness evaluation based on the energy evolution throughout the failure process of rocks. *Journal of Petroleum Science and Engineering, 194*, 107361.

[48]. Altindag, R. (2010). Assessment of some brittleness indexes in rock-drilling efficiency. *Rock Mechanics and Rock Engineering, 43*, 361–370.

[49]. Asadollah, S. N., Aalianvari, A., & Hajialibeigi, H. (2018). Role of geological structures in seepage from Lar dam reservoir. *Arabian Journal of Geosciences, 11*, 632.

[50]. Dursun, A. E., & Gokay, M. K. (2016). Cuttability assessment of selected rocks through different brittleness values. *Rock Mechanics and Rock Engineering, 49*, 1173–1190.

[51]. Wang, P. (2019). Modeling and estimation of production rate in ornamental stones sawing based on brittleness indexes. *Mathematical Problems in Engineering, 2019*, Article 3232517.

[52]. Mikaeil, R., Ataei, M., & Yousefi, R. (2013). Correlation of production rate of ornamental stone with rock brittleness indexes. *Arabian Journal of Geosciences, 6*, 115–121.

[53]. Gunaydin, O., Kahraman, S., & Fener, M. (2004). Sawability prediction of carbonate rocks from brittleness indexes. *Journal of the South African Institute of Mining and Metallurgy, 104*, 239–243.

[54]. Altindag, R., & Guney, A. (2010). Predicting the relationships between brittleness and mechanical properties (UCS, TS and SH) of rocks. *Scientific Research and Essays, 5*, 2107–2118.

[55]. Jiang, J., Wang, D., Han, X., & Di, S. (2020). Relationship between brittleness index and crack initiation stress ratio for different rock types. *Advances in Civil Engineering, 2020*, Article 8091895.

[56]. Zhou, J., Zhang, R., Qiu, Y., & Khandelwal, M. (2023). A true triaxial strength criterion for rocks by gene expression programming. *Journal of Rock*

Mechanics and Geotechnical Engineering, 15, 2508–2520.

[57]. Afrasiabian, B., & Eftekhari, M. (2022). Prediction of mode I fracture toughness of rock using linear multiple regression and gene expression programming. *Journal of Rock Mechanics and Geotechnical Engineering, 14*, 1421–1432.

[58]. Aalianvari, A., Jahanmiri, S., & Abbaszadeh, M. (2024). Developing GEP tree-based, neuro-swarm, and whale optimization models for evaluating groundwater seepage into tunnels: A case study. *Journal of Mining and Environment*.

[59]. Goharzay, M., Noorzad, A., Ardakani, A. M., & Jalal, M. (2017). A worldwide SPT-based soil liquefaction triggering analysis utilizing gene expression programming and Bayesian probabilistic method. *Journal of Rock Mechanics and Geotechnical Engineering, 9*, 683–693.

[60]. Ozbek, A., Unsal, M., & Dikec, A. (2013). Estimating uniaxial compressive strength of rocks using genetic expression programming. *Journal of Rock Mechanics and Geotechnical Engineering, 5*, 325–329.

[61]. Li, Z., Yazdani Bejarbaneh, B., Asteris, P. G., Koopialipoor, M., Armaghani, D. J., & Tahir, M. M. (2021). A hybrid GEP and WOA approach to estimate the optimal penetration rate of TBM in granitic rock mass. *Soft Computing, 25*, 11877–11895.

[62]. El-Kenawy, E.-S. M., Khodadadi, N., Mirjalili, S., Abdelhamid, A. A., Eid, M. M., & Ibrahim, A. (2024). Greylag goose optimization: Nature-inspired optimization algorithm. *Expert Systems with Applications, 238*, 122147.

[63]. Mittal, N., Singh, U., & Sohi, B. S. (2016). Modified Grey Wolf Optimizer for global engineering optimization. *Advances in Computational Intelligence and Its Applications, 2016*, Article 7950348.

[64]. Rabbani, A., Samui, P., & Kumari, S. (2023). A novel hybrid model of augmented grey wolf optimizer and artificial neural network for predicting shear strength of soil. *Modeling Earth Systems and Environment, 9*, 2327–2347.

[65]. Jia, H., Zhou, X., Zhang, J., Abualigah, L., Yildiz, A. R., & Hussien, A. G. (2024). Modified crayfish optimization algorithm for solving multiple engineering application problems. *Artificial Intelligence Review, 57*, 127.

[66]. Chaib, L., Tadj, M., Choucha, A., Khemili, F. Z., & Attia, E.-F. (2024). Improved crayfish optimization algorithm for parameters estimation of photovoltaic models. *Energy Conversion and Management, 313*, 118627.

[67]. Zhang, Y., Liu, P., & Li, Y. (2024). Implementation of an enhanced crayfish optimization algorithm. *Biomimetics, 9*, 341.

[68]. Rana, N., Latiff, M. S. A., Abdulhamid, S. M., & Chiroma, H. (2020). Whale optimization algorithm: A systematic review of contemporary applications, modifications and developments. *Neural Computing and Applications, 32*, 16245–16277.

[69]. Xiao, B., Wang, R., Deng, Y., Yang, Y., & Lu, D. (2024). Simplified crayfish optimization algorithm. In *2024 IEEE 7th Advanced Information Technology, Electronic and Automation Control Conference* (Vol. 7, pp. 392–396). IEEE.

[70]. Bacanin, N., Petrovic, A., Jovanovic, L., Zivkovic, M., Zivkovic, T., & Sarac, M. (2024). Parkinson's disease induced gain freezing detection using gated recurrent units optimized by modified crayfish optimization algorithm. In *2024 5th International Conference on Mobile Computing and Sustainable Informatics* (pp. 1–8). IEEE.

[71]. Patel, V. V., Yadav, A. R., Jain, P., & Cenkeramaddi, L. R. (2024). A systematic kidney tumor segmentation and classification framework using adaptive and attentive-based deep learning networks with improved crayfish optimization algorithm. *IEEE Access*.

[72]. Awadallah, M. A., Braik, M. S., Al-Betar, M. A., & Abu Doush, I. (2023). An enhanced binary artificial rabbits optimization for feature selection in medical diagnosis. *Neural Computing and Applications, 35*, 20013–20068.

[73]. Alamir, N., Kamel, S., Hassan, M. H., & Abdelkader, S. M. (2023). An effective quantum artificial rabbits optimizer for energy management in microgrid considering demand response. *Soft Computing, 27*, 15741–15768.

[74]. Huang, H., Wu, R., Huang, H., Wei, J., Han, Z., Wen, L., & Yuan, Y. (2024). Multi-strategy improved artificial rabbit optimization algorithm based on fusion centroid and elite guidance mechanisms. *Computer Methods in Applied Mechanics and Engineering, 425*, 116915.

[75]. Çetinbaş, İ., Tamyurek, B., & Demirtaş, M. (2023). Parameter extraction of photovoltaic cells and modules by hybrid white shark optimizer and artificial rabbits optimization. *Energy Conversion and Management, 296*, 117621.

[76]. Aalianvari, A., & Jahanmiri, S. (2025). Fluid flow modeling in fractured rocks using human mental search optimization. *Geotechnical and Geological Engineering,* 43(6), 278.

[77]. Abd Elaziz, M., Dahou, A., Mabrouk, A., El-Sappagh, S., & Aseeri, A. O. (2023). An efficient artificial rabbits optimization based on mutation strategy for skin cancer prediction. *Computers in Biology and Medicine, 163*, 107154.

[78]. Riad, A. J., Hasanien, H. M., Turky, R. A., & Yakout, A. H. (2023). Identifying the PEM fuel cell

parameters using artificial rabbits optimization algorithm. *Sustainability, 15*, 4625.

[79]. Alsaiari, A. O., Moustafa, E. B., Alhumade, H., Abulkhair, H., & Elsheikh, A. (2023). A coupled artificial neural network with artificial rabbits optimizer for predicting water productivity of different designs of solar stills. *Advances in Engineering Software, 175*, 103315.

[80]. Chai, T., & Draxler, R. R. (2014). Root mean square error (RMSE) or mean absolute error (MAE)? Arguments against avoiding RMSE in the literature. *Geoscientific Model Development, 7*, 1247–1250.

[81]. Le, L. T., Nguyen, H., Dou, J., & Zhou, J. (2019). A comparative study of PSO-ANN, GA-ANN, ICA-ANN, and ABC-ANN in estimating the heating load of buildings' energy efficiency for smart city planning. *Applied Sciences, 9*, Article 2630.

[82]. Langenbucher, A., Szentmáry, N., Wendelstein, J., Cayless, A., Hoffmann, P., & Gatinel, D. (2025). Performance evaluation of a simple strategy to optimize formula constants for zero mean or minimal standard deviation or root-mean-squared prediction error in intraocular lens power calculation. *American Journal of Ophthalmology, 269*, 282–292.

[83]. Warneke, K., Siegel, S. D., Afonso, J., & Wallot, S. (2025). What the mean absolute percentage error (MAPE) should adopt from Bland–Altman analyses. *German Journal of Exercise and Sport Research*, 1–8.

[84]. Hasanipanah, M., Shahnazar, A., Arab, H., Golzar, S. B., & Amiri, M. (2017). Developing a new hybrid-AI model to predict blast-induced backbreak. *Engineering with Computers, 33*, 349–359.

[85]. Kim, M. S. (2025). Comparative R-squared. *SSRN Electronic Journal*. https://doi.org/10.2139/ssrn.3790200

[86]. Williams, J., Hill, R. R., Pignatiello, J. J., & Chicken, E. (2022). Wavelet analysis of variance box plot. *Journal of Applied Statistics, 49*, 3536–3563.

[87]. Gu, Z., Cao, M., Wang, C., Yu, N., & Qing, H. (2022). Research on mining maximum subsidence prediction based on genetic algorithm combined with XGBoost model. *Sustainability, 14*, Article 10421.

انجمن مهندسی معدن ایران
نشریه مهندسی معدن و محیط زیست
نشانی نشریه: www.jme.shahroodut.ac.ir
دانشگاه صنعتی شاهرود

پیش‌بینی داده‌محور شکنندگی سنگ با استفاده از یادگیری ماشین و الگوریتم‌های بهینه‌سازی پیشرفته

شیرین جهانمیری[۱]، علی عالی انوری[۲*]، مجید نوریان بیدگلی[۱]، و جمال رستمی[۳]

۱. گروه مهندسی معدن، دانشگاه کاشان، کاشان، ایران
۲. گروه مهندسی معدن و مهندسی محیط‌زیست، دانشکده مهندسی، دانشگاه تربیت مدرس، تهران، ایران
۳. گروه مهندسی معدن، دانشکده معادن کلرادو، گلدن، کلرادو، ایالات متحده آمریکا

اطلاعات مقاله

تاریخ ارسال: ۲۰۲۶/۰۵/۰۶
تاریخ داوری: ۲۰۲۶/۰۷/۱۴
تاریخ پذیرش: ۲۰۲۶/۰۸/۰۷

DOI: 10.22044/jme.2026.17675.3514

کلمات کلیدی

ارزیابی شکنندگی سنگ
مهندسی تونل
الگوریتم بهینه‌سازی خرگوش مصنوعی
الگوریتم بهینه‌سازی خرچنگ آب شیرین
تکنیک‌های یادگیری ماشین
مدل‌سازی پیش‌بینی
الگوریتم‌های بهینه‌سازی

چکیده

ارزیابی دقیق شکنندگی سنگ در بسیاری از کاربردهای مهندسی سنگ، به‌ویژه در تونل‌سازی و حفاری‌های زیرزمینی، از اهمیت بالایی برخوردار است؛ زیرا شکنندگی تأثیر قابل‌توجهی بر خردایش سنگ، کارایی عملیات برش و میزان سایش ابزارهای حفاری دارد. بااین‌حال، اندازه‌گیری مستقیم شکنندگی اغلب دشوار، زمان‌بر و پرهزینه است. ازاین‌رو، توسعه مدل‌های پیش‌بینی قابل‌اعتماد بر پایه خواص مکانیکی متداول و در دسترس سنگ، می‌تواند پشتیبان ارزشمندی برای کاربردهای مهندسی باشد. در این پژوهش، چندین روش محاسباتی هوشمند برای پیش‌بینی شاخص شکنندگی سنگ با استفاده از دو پارامتر مکانیکی کلیدی، شامل مقاومت فشاری تک‌محوره و مقاومت کششی به‌کار گرفته شد. برای این منظور، یک مجموعه‌داده جامع شامل ۸۵۴ رکورد از ۲۳ نوع سنگ مختلف، از مطالعات آزمایشگاهی منتشرشده پیشین گردآوری شد. در ادامه، چهار روش پیشرفته مدل‌سازی شامل الگوریتم بهینه‌سازی خرگوش مصنوعی، الگوریتم بهینه‌سازی خرچنگ آب شیرین، بهینه‌ساز گرگ خاکستری و برنامه‌نویسی بیان ژن پیاده‌سازی و از نظر توانایی پیش‌بینی شکنندگی سنگ با یکدیگر مقایسه شدند. عملکرد مدل‌ها با استفاده از شاخص‌های آماری، شامل ضریب تعیین و میانگین قدر مطلق خطا برای هر دو مجموعه‌داده آموزش و آزمون ارزیابی شد. نتایج نشان داد که تمامی مدل‌ها قادر به مدل‌سازی رابطه غیرخطی بین متغیرهای ورودی و شاخص شکنندگی هستند. در میان آن‌ها، مدل ARO بالاترین دقت پیش‌بینی را به دست آورد و با دستیابی به مقادیر تقریبی $R^2 = 0.93$ برای مجموعه آموزش و $R^2 = 0.94$ برای مجموعه آزمون، کمترین میزان خطای پیش‌بینی را ثبت کرد. مدل‌های GWO و GEP نیز نتایج قابل‌اعتماد و رضایت‌بخشی ارائه کردند، در حالی که مدل COA از توانایی پیش‌بینی اندکی پایین‌تر برخوردار بود. یافته‌های این پژوهش نشان‌دهنده کارایی بالای الگوریتم‌های بهینه‌سازی الهام‌گرفته از طبیعت و روش‌های محاسبات تکاملی در مدل‌سازی خواص پیچیده مهندسی سنگ است. مدل‌های توسعه‌یافته، ابزاری کاربردی، کارآمد و قابل‌اعتماد برای برآورد شکنندگی سنگ در شرایطی فراهم می‌کنند که انجام آزمایش‌های مستقیم آزمایشگاهی امکان‌پذیر نباشد و از این طریق می‌توانند به بهبود تصمیم‌گیری در پروژه‌های تونل‌سازی و حفاری سنگ کمک کنند.

نویسنده مسئول مکاتبات: a.aalianvari@modares.ac.ir (علی عالی انوری)